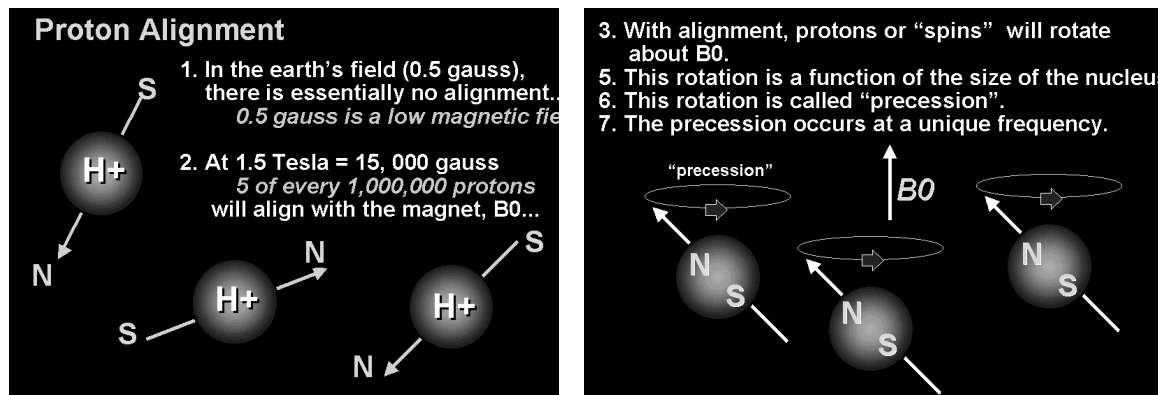


MRI Physics: Basic to Advanced

Mike Moseley, PhD
Department of Radiology
Stanford University CA 94305-5488 USA
<http://www-radiology.stanford.edu>
moseley@stanford.edu

The (very basic) origin of the MR signal Because atomic nuclei such as hydrogen protons are charged, the spinning motion of the proton in a water molecule causes a magnetic moment which is co-linear with the direction of the spinning axis. The spinning proton acts similar to a bar magnet having north and south poles. The strength of this magnetic moment is a property of the type of nucleus and determines the detection sensitivity of MR. Protons possess the strongest magnetic moment, which, together with the high biological abundance of hydrogen, makes it the nucleus of choice for MR imaging.

In the absence of an externally applied magnetic field, the individual protons have no preferred orientation. However, if an externally supplied magnetic field (denoted B_0) is imposed, there is a tendency for the magnetic moments to align with the external field, just like bar magnets would do since the water hydrogen proton has two poles (a dipole nucleus), north and south. A depiction of the proton in a magnetic field is then:



The individual proton magnetic moments (or spins) rotate or more precisely, precess on the surface of a spinning cone. This precessional frequency F is given by a beautifully simple relationship called the Larmor equation, expressed as

$$\text{MRI "Larmor" frequency} = \gamma / 2\pi B_0$$

F is the precessional or rotational frequency, B_0 is the strength of the magnetic field in Tesla or gauss, and γ (g) is related to the strength of the magnetic moment for the type of nucleus considered.

Thus at 1.5 Tesla (= 15,000 Gauss, the field strength of GE Signa)
 $4257 \text{ Hz/gauss} \times 15,000 \text{ Gauss} = 63,855,000 \text{ Hertz} = 63.855 \text{ Megahertz (MHz)}$.

These frequencies are similar to those used by commercial radio and TV stations for FM transmissions to which we are exposed to constantly.

8. At 1.5 Tesla, the precession occurs at 63.9 MHz
 9. The relation between precession rate and magnetic field is the LARMOR equation.
 10. For every 1 Tesla field, precession is 42.6 MHz

Larmor Equation

$$f = \gamma / 2\pi B_0$$

...42.6 MHz/T

Relates precession with magnetic field strength...
 Precession is a frequency...

Linear relation between B0 and frequency...
 Know B0 = know frequency...
 Know frequency = know B0...

In order to detect a MR signal, a condition of resonance needs to be established. The term "resonance" implies alternating absorption and dissipation of energy. Energy absorption is caused by RF perturbation, and energy dissipation is mediated by relaxation processes. Simply put, as mentioned above, irradiation of tissue in a magnetic field with RF energy at the Larmor frequency induces transitions in the protons. *RF energy at other frequencies has no effect whatsoever on the observed protons.*

A summary of the MR spin is given as:

- The magnetic moment cannot be detected w/o a magnetic field
- Protons align in B0, parallel to and against B0
- Alignment in B0 requires a few seconds = T1 is the rate of the re-orientation
- Precession is the term to describe the "spin"
- The rate of precession depends on B0.
- The direction of B0 is given as along "Z" along magnet axis.

The spin of the hydrogen in the magnetic field B0 (typically 0.2 Tesla to 4 Tesla) will nutate or precess in this field, in a way similar to a spinning top on a tabletop. The key to understanding MR is that the rate of this precession is directly affected by the magnetic field strength, B0. Thus, if the magnetic field is altered by a gradient coil, B0 is then altered and the rate of the proton spin immediately changes to match the field strength. To create a signal in MR, we use a brief "radiofrequency" pulse of energy of typically 10-1000 watts. The RF energy oscillates at exactly the Larmor frequency and appears to the spinning protons as a new magnetic field, B1, which is moving at the rate that they are. Protons then are redirected toward this new field. In this, they are "excited" by the perturbation of RF energy and move away from the original steady-state magnetic field, B0.

An applied RF (B1) field is oscillating at 63.9 MHz, at exactly the same rate as the protons in B0.

Protons react to this field B1 since it appears stationary at 63.9 MHz. They react by nutating or flipping away from B0.

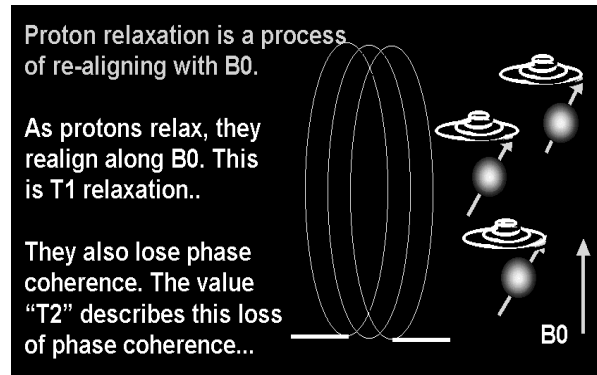
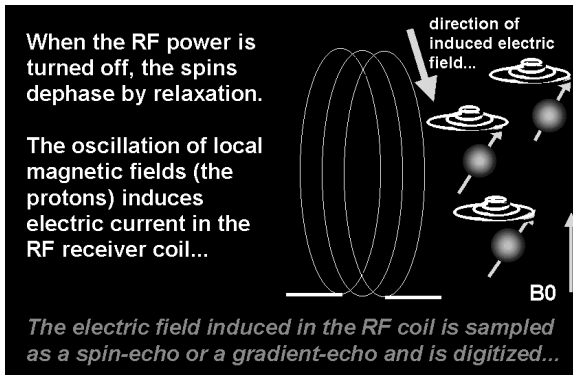
The B1 field appears stationary to the protons because in the "The Rotating Frame" they oscillate at the same frequency...

The RF electric field creates a B1 magnetic field which flips spins away from B0... the "flip" angle will depend on time and power of B1...

This effect is termed RF "excitation"

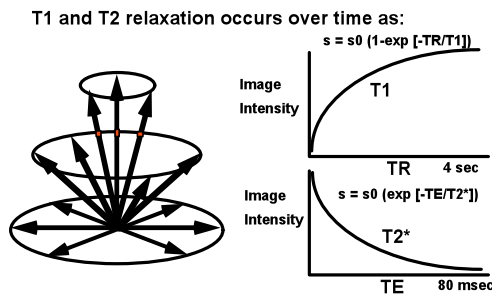
The application of RF energy creates a magnetic field... Every electric field has a magnetic field...

When the FM transmissions or radio frequencies (RF) are turned on by the RF amplifier and sent through the RF coil, the proton magnetization vectors or magnets rotate away from its preferred (or relaxed) axis along B_0 . This flipping of the magnetic angle is proportional to the duration of an RF pulse and the amplitude of the RF. As we will see, flip angles of 90° and 180° are of special importance in imaging. On the sketch below, the vector or arrow represents the spinning moment of the protons aligned along the relaxed or equilibrium axis and the tilting away or flipping of the moment or arrow away from this relaxed axis (below):



Consider the situation immediately after an RF pulse. The net magnetization now lies away from its preferred relaxed axis of spinning and will slowly relax back to this axis. Since this is macroscopic magnetization which is changing direction (rotating) over time, it can induce an alternating (AC) current in a coil of wire, and that current can be used to record the AC action of magnetization in the transverse plane.

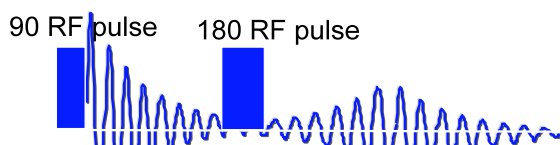
For the protons, the equilibrium orientation is in alignment with the external field B_0 supplied by the superconducting magnet. Once equilibrium conditions have been attained there is no further change unless the system is perturbed. For the protons, this perturbation is in the form of RF energy as dictated by the Larmor equation. The RF perturbation tilts the magnets or proton spins away from equilibrium and the return to equilibrium follows two pathways, called T_1 and T_2 relaxation. As can be seen, the return will have a vertical and horizontal component. These components are called the transverse and longitudinal components and are very unique and inherent for each proton, because the T_1 and T_2 relaxation components or times (the transverse and longitudinal components, respectively) are distinctly determined by the molecular environment of each proton.



How is this relaxation measured? The "how" is called a spin-echo, and it is the basis for the majority of clinical MR imaging. A pulse sequence is a set of RF pulses (and for imaging, field gradient pulses as introduced below in Section D) of defined timing and amplitude which is usually repeated many times, each time resulting in collection of an MR signal. An initial 90° pulse yields a perturbation which decays as a function of T_2 , and then at a time $TE/2$ after the 90° pulse, a 180° RF pulse is applied. After the 180° pulse, a so-called "echo signal" forms, reaching its maximum amplitude at time TE after the initial 90° pulse. The term TE is just the time of

echo and is variable by the technologist operating the scanner. The value of TE is that the image intensity can be weighted by the amount of T_2 relaxation and by the amount of time given for this T_2 process to take place.

A 90-180 spin-echo "pulse sequence":
the loss of phase can be reversed for a time!



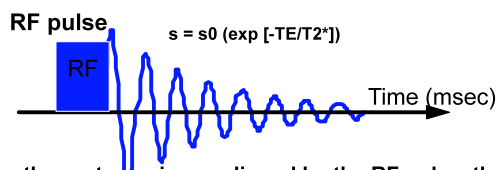
Up to this point, only T2 relaxation has been discussed. A separate process exists which allows the magnets or spins to flip back up to its original axis after being tilted away from equilibrium. This relaxation process is called longitudinal relaxation or T1 relaxation and is also determined by the molecular environment of the proton. Longitudinal relaxation seems to share some of the features observed for transverse relaxation; both are characterized by exponential evolution. In what may be viewed as complementary processes, transverse magnetization *decays*, from maximum to zero, while longitudinal magnetization builds up from zero to maximum. Equilibrium is termed full magnetization and maximum potential for signal. Typical curves are shown below.

We can actually see T1 by image intensity, just as we can see T2 relaxation. For T2 relaxation, we wait a time TE to weigh the image with T2 relaxation; namely, the longer we wait for the signal to form, the longer T2 relaxation has had to occur. A similar parameter, TR is used to weigh the image to T1 relaxation. The longer TR (the repetition time, see above) is, the longer we have let T1 relaxation to restore the proton spins back along the equilibrium axis. Experimentally, this time TR is a delay between repetitions of the 90-180 pulse sequence. This value can be easily set by the operator. Thus, a longer TR would allow more T1 relaxation to take place but would require a longer time.

Spin-echoes: In a spin-echo experiment at 1.5 Tesla, a short burst of radio frequency (RF) energy near the FM band (63.9 MHz) initially excites protons. By applying enough RF power, the net magnetization of the protons is flipped through 90° from its equilibrium alignment along the direction of the main field B0 into the orthogonal *transverse* plane (often called a 90° RF or 90 RF pulse). The excitation affects all protons equally; at the end of the RF pulse, these protons are all in *phase*, that is, they all begin to precess or spin together in rhythm.

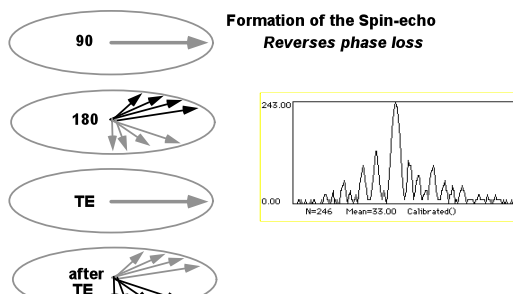
However, very small local variations in the effective magnetic field exist, caused by, among other things, the very presence of the magnetic protons themselves. The nature of the tissue in the magnet determines the local *magnetic susceptibility* or the tendency of the magnetic field to vary. By various processes of proton rotation and diffusion, flow, and motion, during which the protons migrate to different areas of the magnet, the protons will acquire slightly different precession frequencies and so, over time, the initially in-phase spins will progressively *dephase* and the amplitude of the net magnetization will then decrease. This loss of net magnetization or signal decay over time occurs after every RF pulse and follows an exponential decrease, known as the *free induction decay*, with a characteristic time-constant called T2*.

Why do protons lose phase coherence?

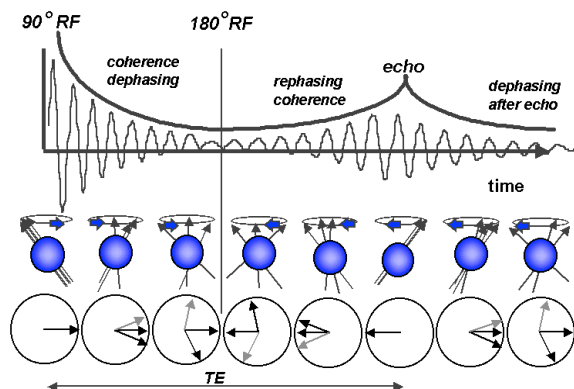


After the proton spin are aligned by the RF pulse, they are in "phase coherence". Phase coherence is lost as the spins diffuse, rotate, and thus experience differing magnetic fields. A magnetic field difference is a measure of T2*

Another way to view the loss of phase coherence that is created immediately after the application of an RF pulse is to consider the phase coherence in the XY plane. This is shown at left.

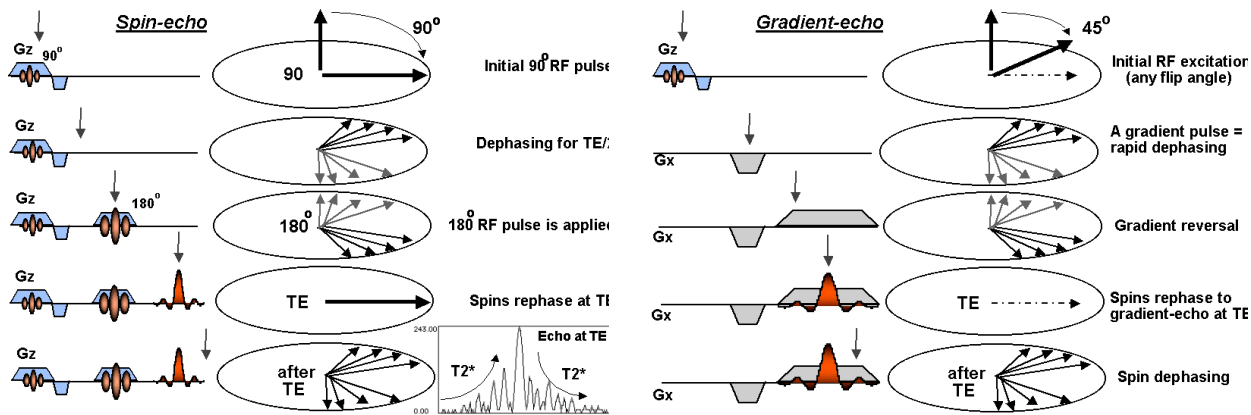


If a refocusing 180° RF pulse (an RF pulse of just twice the power of the initial 90° RF pulse) is applied to these dephasing spins after a time $TE/2$, they will all “flip” over in the transverse plane. After this they continue to precess at the different frequencies according to their local magnetic field, but now instead of progressively dephasing they will progressively rephase to form an echo after an equal precession time. The amplitude of the rephased spin-echo will be attenuated only by the random field fluctuations (characterized by a time-constant, referred to as T_2) that cannot be refocused by use of a 180° RF pulse. The time between the initial 90° RF pulse and the peak of the echo is called TE (“time of the echo”). It is during the *acquisition period*, centered about time TE , which the RF coil detects the RF signal, a microvoltage induced in the RF coil from the proton precession. The use of a spin-echo has the primary advantages of collecting the signal after a designated time (TE) to allow for T_2 -weighting and to create time delays in the pulse sequence to allow the gradient pulses required for image formation to be turned on and off, a process that can require several milliseconds.



The time between the initial 90° RF pulse and the peak of the echo is called TE (“time of the echo”). It is during the *acquisition period*, centered about time TE , which the RF coil detects the RF signal, a microvoltage induced in the RF coil from the proton precession. The use of a spin-echo has the primary advantages of collecting the signal after a designated time (TE) to allow for T_2 -weighting and to

create time delays in the pulse sequence to allow the gradient pulses required for image formation to be turned on and off, a process that can require several milliseconds. The processes of the spin echo and the gradient echoes are similar in design but vastly different in the physiological ramifications (see section below on magnetic susceptibility).



Building Blocks of MRI To repeat, there are three events that occur during the imaging experiment, each event using a separate set of gradient coils corresponding to the three magnet axes. All imaging experiments are identical except for which gradient is used for which event.

First, a slice is created with a 90° RF pulse and a gradient pulse from the slice selection gradient. The slice-selection gradient can be the x, y, or z gradient, depending on whether the operator desires an axial, sagittal, or coronal scan. This event is followed at a time $TE/2$ with an identical RF/gradient pulse set,

using this time however, a 180° RF pulse, the purpose of which is to refocus the dephasing following the initial 90° pulse and thus to form a spin-echo within the slice.

Between the 90 and 180 RF pulses, a "phase-encoding" gradient pulse of differing gradient strength is applied for a few milliseconds. This gradient pulse uses a different gradient coil than the slice-selection event. At the time TE (or "time of echo"), the remaining third gradient coil is turned on while the spin-echo is evolving. Also, during this time, the RF coil listens or receives the created spin-echo. By receiving the echo signal, the computer is digitizing the current induced in the RF coil from the evolution of the spin-echo. This event is termed the "readout" or "frequency-encoding" of the echo signal.

It is important to understand the relation of the actions of the gradient coils outlined above. If the z gradient coil is used with the RF pulses, then the resulting image created will be that of an "axial" image. In this axial image then, the phase-encoding and frequency-encoding events must employ the x and y gradient coils. Similarly, if the y gradient coil is used to create the slice and the x and z gradient coils are used to phase-encode and frequency-encode the resulting echo, then this image orientation will be a "coronal" image. Finally, if the x gradient is used with the RF pulses to create the slice, then the resulting image orientation will be that of a "sagittal" image. By visualizing the direction of the gradient coils and the magnet axes, the image orientation of axial, sagittal, and coronal scans becomes clear.

Diagrams of the RF and gradient pulses are used to denote the sequence of events that occur during the imaging experiment. These diagrams are known as pulse sequences. The complete pulse sequence for the spin-echo imaging experiment is shown below.

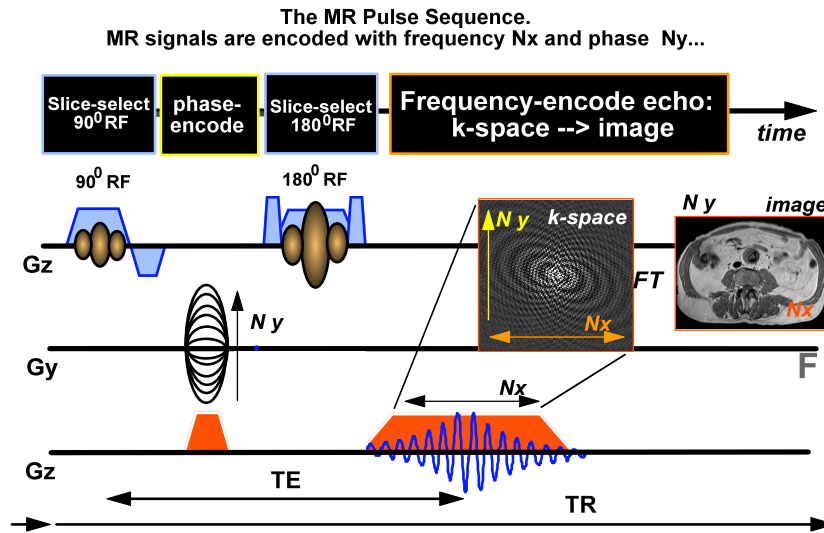
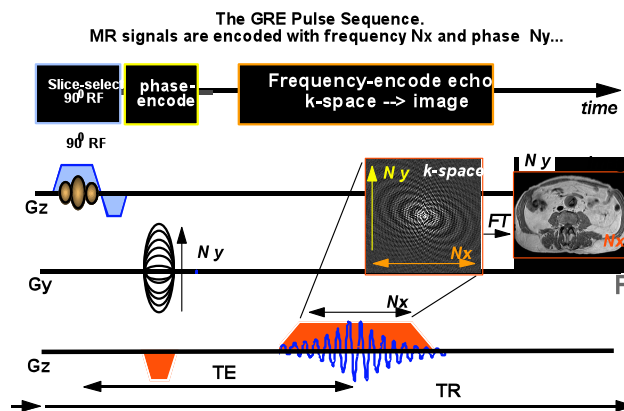


FIGURE. The complete spin-echo MRI pulse timing diagram (pulse sequence) is shown above. In all pulse sequence diagrams, the horizontal axis is the time axis; that is, what events occur as a function of time. In this sequence, the slice-selection gradient is turned on at the same time as the 90° RF pulse is applied to the spins. After a brief delay, the phase-encoding gradient is turned on with a variable strength (giving this event a step-ladder appearance); this strength is varied in 128 or 256 steps depending on the desired resolution of the image. The 180° RF pulse and slice-selection gradient is then applied at a time TE/2. For the detection and frequency-encoding of the spin-echo, the frequency-encoding gradient is turned on while the echo is detected from the RF coil. All gradient coils are kept off until turned on. The ramping appearance of the gradient pulses is just that; the gradients are gradually turned off to avoid excessive eddy currents induced in the main field B₀. This ramp is usually 1-2 msec long. The delay time TR (or to help remember, the "time of repetition") is that time between the sequential applications of the 90° RF pulse. The

total scan time for the above sequence is equal to the product of TR X NEX (number of signal acquisitions) X Number of phase-encoding steps (usually 128, 192 or 256). The delay time **TE** (or the "time of echo") is that time between the 90 RF pulse and the frequency-encoding (or readout) of the spin-echo. TR and TE are varied to allow for the relaxation times T1 and T2 to produce the desired contrast in the MR image.

The horizontal axis in a pulse sequence is that of time. The various lines of those of each of the gradient coils and the RF coil. Thus for example, during the 90 slice event, only the slice-selection gradient (be it x, y, or z, depending of the desired image orientation) and the RF coil is on (or transmitting). During frequency-encoding, only the frequency-encoding gradient is pulsed on while the RF coil is receiving the signal which the computer then digitizes and stores in memory.

The corresponding sequence for the gradient-echo MR sequence is given below and differs from the spin-echo sequence by the inclusion of only one RF pulse. The gradient-echo sequence uses the reversal of the magnetic field itself to form a field echo instead of a spin-echo. Either one can be used for MRI.



MRI and Tissue Contrast Mechanisms. Lesion detection depends primarily on identifying abnormalities of morphology and/or signal intensity. MR sequences provide images with good spatial resolution and contrast while dealing with inevitable trade-offs in coverage and imaging scan time. This becomes then a subjective blend of *signal-to-noise* (SNR) considerations and the underlying *contrast* between tissues. The observed SNR and the MR Voxel resolution depend on the slice thickness (ST), field-of-view (FOV), and the matrix size. So, typically, for a FOV of 20 cm, matrix size of 256x256 pixels and ST= 5 mm, there would be 65536 voxels each measuring 0.8 by 0.8 by 5.0 mm in size.

The intensity, or brightness, of the voxel reflects the amplitude of the MR signal arising from that voxel. It is the intrinsic "relaxation time" parameters of the tissue, characterized by the relaxation times T1 and T2, together with the proton density N (H) that provide the source for establishing tissue contrast-to-noise. The relaxation times T1 and T2 differ greatly in tissues. For pure water T1 = T2, whereas in all tissues T1 > T2, though the variation in T2 in pathological situations is greater. Images contrasting changes in T2 are usually most sensitive in detecting and characterizing pathology. An important caveat in wound healing is that the alteration in tissue contrast afforded by MR contrast agents is greater for T1 times.

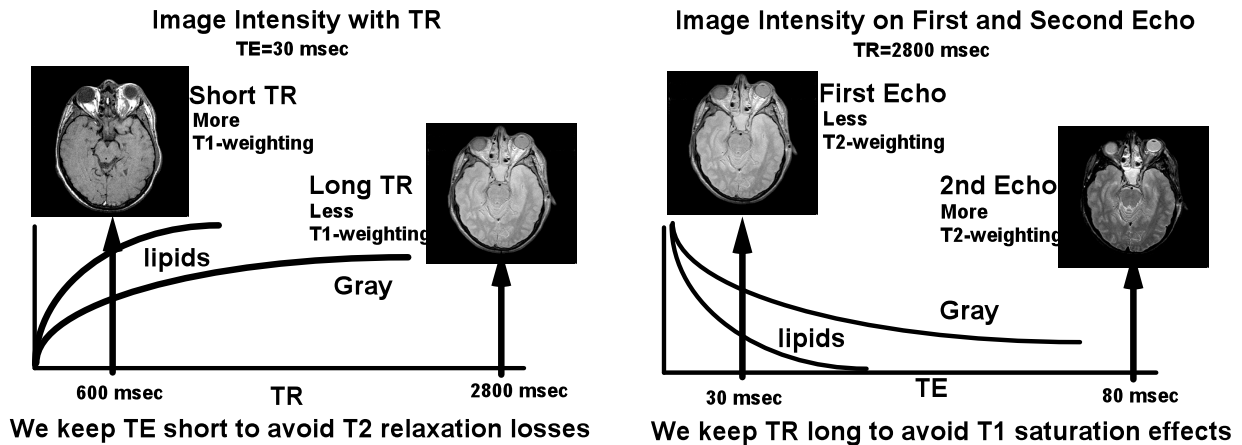
The relaxation time-constant T2 describes net magnetization loss between proton excitation and the echo acquisition (the MR signal is usually detected as a "spin-echo"). If this echo time, TE, is made longer, the spin-echo amplitude decreases. The spin-echo image is acquired from a series of 192-256 views, each separated by a repetition time TR. During TR, protons are allowed to "relax" or realign by a rising exponential time constant T1 along the direction of a constant main magnetic field (at 1.5 Tesla or 15,000 gauss, for example). If TR is made short to reduce scan time, those protons with long T1's will not have

enough time to fully recover and will not contribute signal to the next view and the echo amplitude will be reduced.

Because there are two tissue relaxation times, T1 and T2, together with TR and TE, there are four basic image types. These are:

- Σ Long TR, long TE T2 influence dominant (T2-weighted).
- Σ Short TR, short TE T1 influence dominant (T1-weighted).
- Σ Long TR, short TE Neither T1 nor T2 influencing (Proton density).
- Σ Short TR, long TE Both T1 and T2 influencing (not used).

A summary of this is shown below:

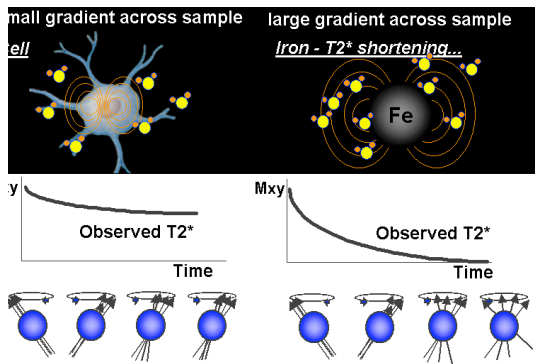


To understand the role of TE and image contrast, as TE is increased, the signal and the image become more T2-weighted. There exist many other potentially useful tissue contrast mechanisms in MR imaging suitable for mapping pathology over underlying anatomy. These mechanisms will be discussed in the follow-up lecture and include:

Phase Coherence and MR Signal Intensity. Perhaps the single most difficult concept to understand in MR is that of "phase coherence". Immediately following the initiating RF pulse ("alpha"), such as the 90° pulse in the spin-echo sequence or a partial flip angle pulse in gradient-echo sequences, all the protons excited within the slice are aligned in the same direction. That means that they all were excited by the same amount. They are for that one moment precessing together, at the same rate. This "togetherness" of all these protons precessing at the same rate is called "phase coherence". The term phase refers to the "amount" of togetherness. Groups of protons lose phase coherence when they diffuse, perfuse, or flow away from one another to differing magnetic fields. By moving to a different magnetic field, their precessional frequency changes and consequently, they lose togetherness or phase. When the protons are aligned together precessing at the same rate after any RF pulse, their individual contributions to the receiver signal are additive; that is, they all contribute to the signal. Over time, however, the phase coherence is lost exponentially (see above). The phase coherence is maximized just after the initial RF pulse and then decays away in a process of dephasing.

As the spins rotate or diffuse from one region within the slice to another, they lose their coherence because of very small local variations in the effective magnetic field, caused by the very presence of the magnetic protons themselves, among other things (such as the presence of metal or air-tissue interfaces). The nature and the composition of the tissue determine the local *magnetic susceptibility* or the degree to which the

magnetic field is altered by the tissue. When the field is heterogeneous, the spins' resonant frequencies are also. As time goes by, the signals from spins at different frequencies become more and more out of phase with each other and the net signal of the ensemble decreases. The rate of this time-dependent phase loss is determined by the microenvironment of the proton (such as the tissue T₂, the field homogeneity, chemical shifts of the spins and their diffusion rates). The time course of this loss is termed the "free induction decay" or the FID. It is this decay or loss of phase coherence that is characterized by the T₂^{*} term. T₂^{*} is the combined effect of T₂ relaxation (spin-spin interaction) and T₂' ("T₂ prime"); T₂' refers to off-resonance effects which include magnetic susceptibility and local B₀ inhomogeneities.



The loss of phase coherence due to T₂' can be refocused with an RF pulse. If a refocusing 180° RF pulse (with twice the amplitude of the initial 90° RF pulse) is applied following an initial 90° RF pulse, the spin phases will now “flip” over in the transverse plane and will progressively “rephase” to form an echo after an equal precession time. The amplitude of the rephased “spin-echo” will be exponentially attenuated by random B₀ fluctuations (characterized by a time-constant T₂) that cannot be refocused by use of a 180° RF pulse. The time between the initial 90° RF pulse and the rephasing

of the echo is called *TE* (“time of the echo”). It is during this *sampling* or acquisition period, centered for several milliseconds about the echo time TE, that small voltage fluctuations induced in the RF coil is digitized to acquire the echo signal.

The concept of the 90° RF and the 180° RF to form a spin-echo is well-known. The application of additional 180° RF pulses can be serially applied to form a train of spin-echoes. This difference between T₂ and T₂^{*} often separates the apparent tissue contrast between the spin-echo sequence (where the T₂ loss is observed) from the corresponding gradient-echo sequence (where the echo is formed not from RF but from the applied magnetic field gradient itself; i.e., gradient reversal). Gradient pulses are used everywhere to alter, create and crush the MR signal, and are a part of all slice-selection, frequency-encoding, and phase-encoding processes.

Functional Neuroimaging. The world of neuroimaging once familiar to the practicing Neuroradiologist is rapidly changing. The traditional focus on neuroimaging has been built primarily on the technological advancement of non-invasive imaging modalities such as CT, US, and MRI. However, a new focus is being placed on the acquisition of new kinds of information acquired from traditional modalities. The traditional world of neuroanatomic imaging and interpretation is being rapidly altered with the advance of sophisticated functional neuroanatomic imaging techniques. The pace of technical innovation and a wide range of functional neuroanatomic applications in many aspects of neuroimaging present unique challenges and exciting opportunities for the practicing neuroradiologist. While the picture of the neuroradiologist has been that of performance and interpretation of radiologic examinations, the neuroradiologist of tomorrow will be called upon for combined interpretations of traditional neuroanatomy with dynamic functional neurophysiology overlaid upon the anatomy.

Functional MRI has come to encompass such diverse areas as the physics of high-speed imaging, the microenvironment of the water protons, flow and motion as well as the physiological principles of the water protons, blood oxygenation level dependent imaging, dynamics of cerebral hemodynamics, the many pathways of intracellular metabolism, the spatial and temporal dynamics of cortical activation, as well as

intravascular and tagged MR contrast agents. The while the pace of functional MRI continues to accelerate, the practicing MR specialist is being presented with interpretations of many various functional exams.

The rapid pace of functional neuroimaging has created a situation in which the technical ability of MRI to evaluate function is far ahead of the understanding of any one discipline for the value and everyday utility of the modality. The frantic development of new functional MRI techniques has created enormous wealth to a variety of groups in neuroimaging. It would also be safe to say there are no disciplines in neuroscience which are clearly ahead of others at this present time, although many disciplines are working hard to change that.

Magnetic resonance imaging (MRI) has been established for over a decade as a superior research and clinical modality for anatomical imaging. Noteworthy for exceptionally good sub-millimeter spatial and sub-second temporal resolution, MRI is now demonstrating the potential of tracing the links between tissue function, metabolism, blood flow and hemodynamics in both normal and disease states. Functional magnetic resonance imaging (fMRI) can utilize conventional MRI technology and equipment to image the intrinsic hemodynamic and metabolic changes that may occur in human cognitive functions such as vision, motor skills, language, and memory and indeed in all mental processes. These techniques have also revolutionized detection of disease states such as stroke. MRI can within minutes acquire functional images non-invasively from an individual in any plane or volume at comparatively high-resolutions and then overlay observed functional centers of activation onto the underlying cerebral anatomy, imaged with the same MRI scanner. FMRI is rapidly evolving beyond the localization of visual, motor, and somatosensory responses to use in respective surgery of tumors, localization of “handedness”, and elucidation of brain function and metabolism altered by pathologies such as stroke. Given the large number of clinical MRI scanners operating worldwide, fMRI will give rise to routine clinical assessment of brain and organ function, in addition to the anatomical imaging roles of present-day MRI.

Much of the recent progress in MRI has come because of “high-speed” imaging capabilities. This typically means that enhanced gradient strengths are used to produce images in one or a few “shots” or echo-trains. Echo-planar and spiral imaging are two variations of a high-speed gradient-echo MRI technique, although many other methods exist. Spin-echo variations of high-speed imaging fall into the class of “fast spin-echo” MRI. High-speed MRI suggests that images are acquired in a few seconds or less, and provide the means of acquiring motion-free images (for diffusion MRI to reduce patient motion and the effects on image artifacts) or a series of rapidly-acquired images to follow or “track” the progress or time course of a bolus of injected contrast agent or of a slab of inverted or saturated arterial blood protons (for perfusion MRI).

Fast Spin Echo

A variant of the conventional spin-echo (CSE) sequence has appeared and has brought a quiet revolution to body, musculoskeletal and CNS MRI. This more rapid spin echo sequence differs from CSE imaging in the way that it traverses k-space. In our discussion here, we will refer to the rapid spin echo sequence as Fast Spin Echo (FSE), originally introduced as RARE and also called TurboSE (TSE). FSE or RARE imaging can be done in a number of shots (for higher resolution) or in a single-shot (for speed while reducing susceptibility artifacts).

Remember that CSE obtains one view from only one spin-echo per repetition time TR. The scan time is determined by the product of the repetition time (TR), the number of phase-encoding steps and the number of signals averaged (NSA). In FSE a train of multiple spin-echoes is generated from multiple 180° RF pulses which are close enough together (with small echo spacings on the order of 17 msec) to provide multiple views from a single 90° RF excitation. Imaging time is shortened by a factor of the number of echoes in the train that are collected, which can vary up to 64 echoes acquired per train. The general FSE pulse sequence is compared to its CSE cousin.

The appeal of FSE lies, of course, in the potential to significantly reduce scan times, which reduces motion artifact and increases patient comfort and throughput. Breath-held FSE exams are now possible. Further, scan time can also be traded for higher resolution and/or the increase in NSA (NEX). The acquisition of multiple phase-encoding steps per TR can be used to acquire images of very high resolution in realistic times by acquiring up to 512 phased views. Conversely, high resolution images can be acquired at conventional spatial encoding values but at a significant reduction in the size of the field-of-view which can necessitate an increase in NSA now more easily allowed at faster acquisition times. FSE in combination with phased array coil systems may lead to routine high resolution body imaging.

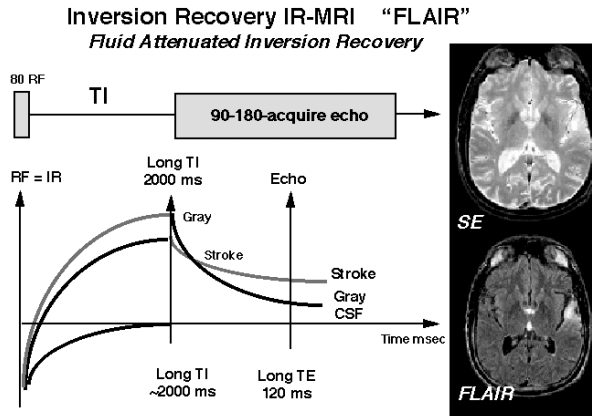
FLAIR FSE

FSE has become important recently in that inversion-recovery (FLAIR) methods have made neuro imaging easier in depicting abnormalities in tissue T₂, such as in stroke. The use of FLAIR is of great interest in neuro MRI. Current imaging techniques (CT or conventional MR) are hampered by an inability to image changes in the early time period following ischemic insults. T₂-weighted MR images, obtained during the late stages of the evolution of cerebral infarction, correlate well with the histopathology of the lesion. However, conventional SE T₂-weighted MRI is insensitive to ischemic tissue damage before significant vasogenic edema develops, requiring repeated scanning to confirm the initial neurological assessment of acute ischemia. The poor conspicuity of acute ischemia on conventional T₂-weighted SE or fast spin-echo (FSE) MRI is largely due to the very subtle changes occurring in the parenchymal T₂ and to the hyperintense signal from cerebrospinal fluid (CSF) masking subtle pathology. To suppress this masking by CSF, an inversion pulse can be used with an appropriate inversion time (TI) to render CSF hypointense in brain, and bring out the subtle changes in brain T₁ and T₂ with an increased dynamic range. An IR sequence with a long TE, termed "FLAIR", has potential in the detection of subtle T₂ changes. Thus, FLAIR may prove to be complementary with DWI and perfusion MRI in detecting pathology such as subarachnoid hemorrhage or stroke (1-3).

By suppressing adjacent CSF signal and emphasizing T₂ weighting, FLAIR proved more sensitive in detecting infarcts than conventional T₂-weighted images. This is shown in the Figure below comparing FLAIR with T₂ in a patient presenting with a stroke symptoms 3 weeks earlier. Here, while FLAIR nicely outlines white matter disease, the DWI images show no observable hyperintensity which would indicate any acute stroke effects. The ADC maps created from the T₂ and the DWI images shows the periventricular white matter regions to possess very high ADC values, much higher than normal, suggesting a high water content and fast proton diffusion.

For acute stroke, however, we are finding that DWI detected acute infarcts earlier than either FLAIR or T₂-weighted images and was able to differentiate acute from chronic by virtue of the apparent diffusion (ADC) maps. This ability of DWI to better delineate early stroke better than T₂ or FLAIR is shown in Figure 2, in which a 24 hour stroke was suspected in the brainstem.

The use of "inversion-recovery" methods is therefore of great interest in neuro MRI, by making it easier to depict abnormalities in tissue T₂, such as in stroke (1-3). The inversion recovery method uses an initial 180° pulse to suppress the usually strong signal from CSF; that is, an inversion pulse can be used with an appropriate inversion time (TI) to render CSF hypointense in brain, and bring out the subtle changes in brain T₁ and T₂ with an increased dynamic range. An IR sequence with a long TE, termed "FLAIR" of "FLuid Attenuated Inversion Recovery", has potential in the detection of subtle T₂ changes. Thus, FLAIR may prove to be complementary with DWI and perfusion MRI in detecting pathology such as subarachnoid hemorrhage or stroke (**below**).



Left. FLAIR FSE in stroke. The purpose of the initial 1800 RF pulse is to place all of the magnetization along the Z axis, the recovery of which depends on the relaxation time T1. As CSF protons cross the zero-magnetization (that is, the net magnetization is zero), the 900-1800 sequence is started. At this point, no CSF protons are excited (since they have zero magnetization) and CSF seems suppressed in the resulting image. All other protons are seen. This tends to mask CSF from pathology protons, such as those found in infarction. They have shorter T1's than CSF and are not suppressed. This aids in the depiction of the lesion, provided that the T2 is elevated and that the T1 is not as long as that found in CSF.

By suppressing adjacent CSF signal and emphasizing T2 weighting, FLAIR proved more sensitive in detecting infarcts than conventional T2-weighted images (above). For acute stroke, however, we are finding that “diffusion weighted imaging” (DWI) detects acute infarcts earlier than either FLAIR or T2-weighted images and was able to differentiate acute from chronic by virtue of the apparent diffusion coefficient (ADC) maps. A discussion of DWI and the method to acquire DWI images, EPI, follows below.

Single-shot FLAIR

Recently, FSE has been improved to produce SE images in a single-shot. This will have an immense impact on the future of MRI as many new applications requiring the superior image quality of SE MRI can be done in a fraction of the time that even FSE has required. Recently, a variant of the single-shot FSE diffusion-weighted sequence has been perfected and compared to that shown above. The addition of the diffusion-weighting makes the ssFSE sequence near ideal for rapid imaging of acute stroke, a topic covered below using single-shot EPI instead of ssFSE.

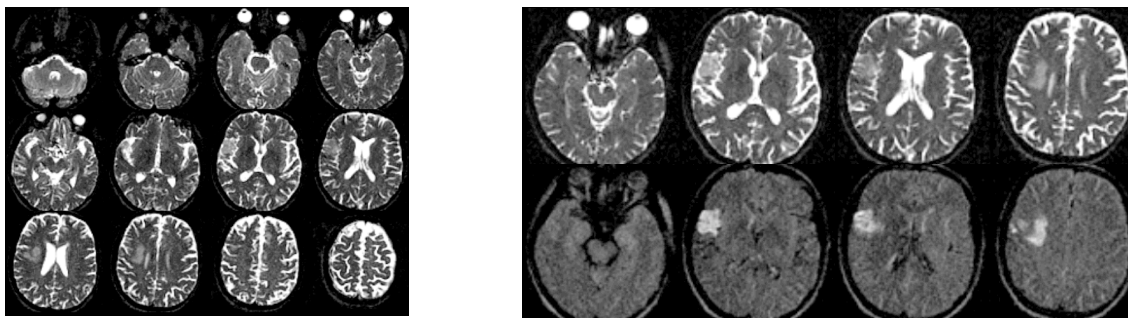
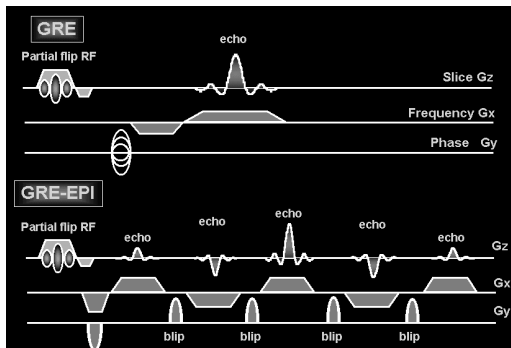


Figure: Single-shot T2-weighted FSE images. Each image requires only 350 msec to acquire. Multi-slice images can be acquired in a sequential fashion. Top right: Single-shot T2-weighted images (top row) and diffusion-weighted images (bottom row). The acute lesions are easily depicted using the diffusion-weighting filter for the ssFSE images.

High-speed Imaging – EPI. MR echo-planar imaging (EPI) methods have existed since the late 1970’s. The concept of echo-planar imaging lays in the acquisition of a complete set of gradient-recalled multiple echoes within a single-shot time of 32-144 msec. It is not unreasonable to consider that EPI is to gradient-echoes what Fast Spin Echo is to conventional spin-echo methods. The noted exception is that a continuous or pulsed (“blipped”) phase-altering gradient is applied simultaneously with a series of rapidly-switched gradient-recalling pulses (think of this as repeated gradient-recalled-echoes to form a multi-echo train) during the conventional echo sampling time. During this time, typically 32-64 msec, the gradient is

switched often enough to form 64 to 128 echoes. Single-shot imaging requires a frequency- and phase-encoding gradient-pulsing scheme which covers the frequency-phase space (k-space) in a single burst of radio frequency and gradient pulses within one TR period. To do this rapidly, both EPI and spiral use repeated gradient-echoes to advance the frequency- and phase-encoding, which can create significant T2*-induced artifacts.



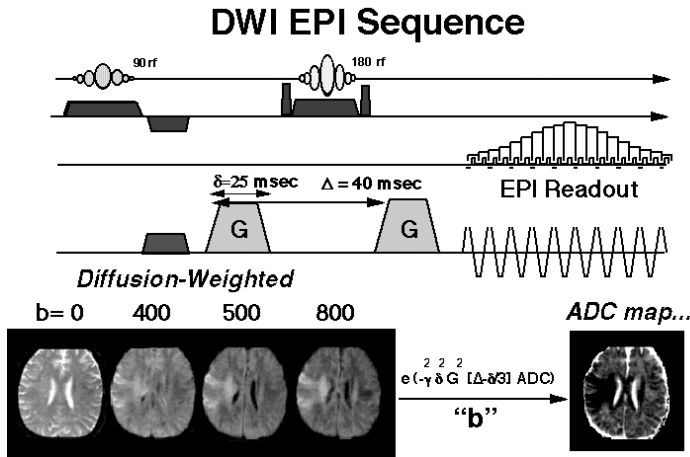
Left: Needless to say, the hardware necessary to collect good echo-planar images requires both strong eddy-free gradients (typically > 1 gauss/cm) with rise and fall times of < 0.1 msec and a very fast analog-to-digital digitizer which can sample repeated gradient-recalled-echoes (with typical durations of 500 microseconds to 1 msec) over the 32 to 64 msec sampling time. In practice, series of images can be acquired within seconds, making bolus-tracking, quantitation of diffusion, flow patterns, and functional task activation readily visible in near real-time. Today, numerous sites have these “upgrades” with many more being planned.

It is the rapid acquisition of a train of gradient-recalled-echoes that identifies the EPI sequence. The initial magnetization can be prepared in any number of ways. Prior to acquisition of the gradient-recalled-echoes, a 90° - 180° spin-echo pulse sequence can be applied or a partial-flip RF pulse could be applied. This makes EPI compatible with spin-echo, gradient-recalled-echo, inversion-recovery, diffusion-weighting, fat saturation, spatial saturation, all of course in a single-slice or multi-slice mode.

Functional Imaging: Proton Diffusion Weighted Imaging (DWI). The MR image intensity can be altered by the number of hydrogen nuclei within a pixel (flow-modulated proton density), proton relaxation rates, diffusion, blood flow and perfusion, and by transient or permanent alterations in the local magnetic field surrounding a tissue. Since many contrast mechanisms are present, diagnostic tissue contrast is a process of isolating one or more of the active mechanisms.

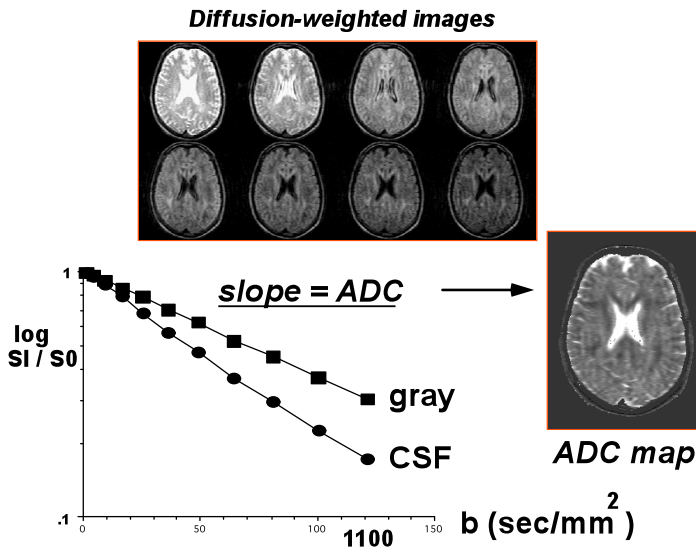
Several novel and significant tissue contrast mechanisms have been described within the last 5 years that are sensitive enough to image the effects of function. Intrinsic velocity and phase change contrast can be used to image MR angiography. Similarly, mapping of proton diffusion in tissues has continued to inspire and impact new methods to rapidly and non-invasively detect and characterize cerebral stroke. This one functional method alone has revolutionized clinical neuroscience, particularly since diffusion mirrors changes in the microenvironment of water, which dynamically change with metabolic alterations.

To date, most diffusion-weighted MRI sequences have been based upon spin-echo Stejskal-Tanner (ST) techniques. Since the two ST diffusion-sensitizing gradient pulses are symmetrical (same length, amplitude and position with respect to the RF pulses) and separated by a 180° RF pulse, all proton spin-dephasing caused by the first diffusion-sensitizing gradient pulse will be refocused (spin-rephased) by the second diffusion-sensitizing gradient pulse for stationary spins. Randomly-moving spins (because of flow, perfusion, diffusion, etc.) do not completely refocus and will decrease the received spin-echo. As the gradient strength is increased the loss due to the apparent diffusion coefficient (ADC) is greater and the diffusion-weighted images become darker by an amount described by the ADC. One way to map the ADC is to acquire a series of increasing diffusion-weighted b-value images in a row. The slope of the image loss is the ADC.



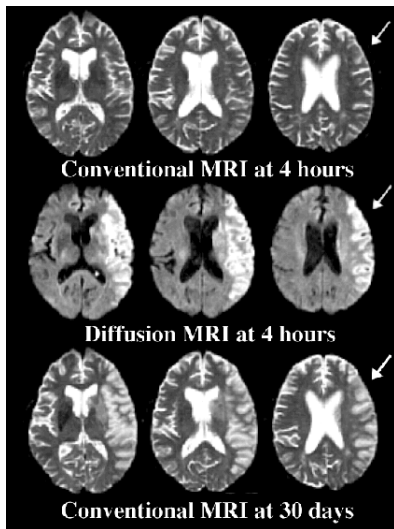
Left. Diffusion MRI. Given a typical spin-echo EPI sequence, the addition of the two matched gradients along any of the three axes allows one to dephase and then rephase all protons within a slice. Those protons diffusing between the two matched gradient pulses lose phase coherence with those protons not moving and drop out from the signal. This sensitivity can be adjusted by the strength of the diffusion-sensitizing gradients and can be used to quantitatively measure the apparent diffusion coefficient (ADC). In stroke, those protons in ischemic regions slow down and this becomes very apparent on diffusion-weighted images as regional hyperintensity.

Left: A typical measurement of apparent diffusion from MR images requires plotting the natural logarithm of the image intensities against the b-value. The slope of this line directly yields the apparent diffusion coefficient, ADC.



The diffusion sequence maps proton displacements expressed by an apparent diffusion coefficient, ADC (usually given in cm^2/sec or m^2/sec). For a typical proton diffusion coefficient, ADC, of $1 \times 10^{-5} \text{ cm}^2/\text{sec}$ in gray matter, the average displacement along one direction becomes 8-9 microns, observed over an observation time, t , of 30-50 msec.

Diffusion-weighted imaging (DWI) is becoming widely used clinically by being capable of imaging ischemia-induced changes in water protons within minutes after an insult (8-11) (**below**).



Left Detection of early brain attack. MRI images of a 55 y.o.m. 4 hours after onset acute symptoms. Top row: Conventional T2-weighted MRI images taken at 4 hours from 3 different slices of the brain show no clear depiction of the stroke (arrow), and could not confirm the neurological assessment of a serious brain attack. Middle: Corresponding DWI images taken also at 4 hours now clearly show the extent of this very large and serious brain attack (arrow), extending over almost the entire hemisphere. Lower row: Conventional T2-weighted MRI images from same 3 different slices taken now at 30 days confirm the early assessment from DWI by showing the final size of the stroke (arrow). Early confirmation of the presence and extend of a brain attack at presentation will dramatically influence the course of action for patient management.

This utility of DWI lays in the fact that water apparent diffusion is measurably slower in regions of ischemia compared to normal brain with ADC decreases of 30%-60% reported in experimental studies. These regional decreases were correlated with total or near-total perfusion deficits; the ADC does not decrease until cerebral blood flow drops below a perfusion threshold of 15-20 ml/100 gm/min, implying the existence of a perfusion threshold. Following permanent occlusions, ADC decreases are highly correlated with the areas of infarction measured by later histopathology. Initial reports and recent findings suggest that significant apparent diffusion slowing (ADC decreases) in ischemia reflects a shift of relatively more mobile extracellular water protons into a more hindered intracellular environment perhaps coupled with cellular membrane changes. The apparent decrease in ADC post-occlusion suggests that apparent diffusion is coupled to metabolic processes rather than to motion mechanisms, reinforced by recent reports of ADC decreases observed in models of status epilepticus, administration of intraparenchymal ouabain, and cortical spreading depression.

Needless to say, DWI studies in humans have become the focus of intense studies. Patient studies have been performed much later after presentation than the imaging studies performed in the previously described animal models of ischemia, with infarcts ranging between 2 hours to four years in age. The number of patients studied to date by a number of investigators has led to an understanding of how the ADC changes over time, from acute values much below normal that later rise to values much higher than normal. Today, DWI is well on the way to becoming a surrogate endpoint for clinical assessment of cerebral ischemia by acquiring the most critical information possible, the presence or absence of an occlusive event, the circulation and location of the event, and the extent of the event.

Functional Imaging of the Brain, Diffusion Tensor Imaging (DTI). Diffusion tensor imaging (DTI) is a promising new technique for the assessment of white matter (WM) structural integrity and connectivity. The movement of water in brain is hindered by the presence of cell membranes, myelin sheaths surrounding axons, and other structures, particularly so in white matter tracts where the apparent water diffusion is highly anisotropic, since diffusion parallel to axons and myelin bundles is considerably faster than that perpendicular to the axons. Tensors (a mathematical construct useful for describing multidimensional vector systems) are ideal for describing proton diffusion restricted by white matter tracts, by indicating the direction and the magnitude of restriction. This in turn offers an index of directional coherence of fiber tracts or integrity of cellular structure. Based on the diffusion tensor, several quantitative and absolute measures can be determined and mapped, such as the apparent diffusion coefficient (ADC), the degree of anisotropy (e.g., fractional anisotropy, FA) and measures of the correlation in orientation between a given pixel and its surrounding neighbors (e.g., the lattice anisotropy, LA). Over the past decade, diffusion weighted imaging has become an important image modality in the clinical management of stroke

and for investigation of mechanisms of neuronal damage in animal models of cerebral ischemia, and the diffusion weighted images or the ADC maps are evaluated routinely. However, despite the fact that Wallerian degeneration has been shown to decrease the degree of anisotropic water motion in peripheral nerve and DTI imaging has demonstrated a decrease in anisotropy in stroke patients, tensor measures have not yet become an integral part of clinical studies.

Our diffusion tensor imaging protocol is performed on a 1.5T Signa (GE Signa Horizon EchoSpeed) using a spin echo EPI technique (FOV 24cm, 128x128 zero-filled to 256x256; TE/TR = 106ms/6s, 18 oblique slices, slice thickness 5mm skip 0mm). The amplitude of the diffusion-sensitizing gradients was 1.4Gauss/cm with a duration and separation of 32ms and 34ms, respectively. This resulted in a b-value of 860s/mm². Diffusion was measured along six non-collinear directions. For each gradient direction, four images were acquired and averaged. Two images with no diffusion weighting (b = 0s/mm²) were acquired and a set of Inversion Recovery (IR) images for CSF nulling (TI ~ 2100ms) were acquired with b = 0s/mm²; these images were used to unwarped the diffusion weighted images, which resulted in a more robust unwarped than using the non-IR b=0 images. The acquired images were reconstructed prior to averaging, giving NEX = 4 for the high b-value and NEX = 2 for b = 0s/mm². The diffusion tensor was determined for each pixel after which eigenvalues, eigenvectors and the FA was calculated.

Diffusion “Anisotropy” Methods and Application to Neurologic Diseases. We have added DTI to a wide variety of brain MR protocols such as acute and chronic stroke, trauma, multiple sclerosis, premature babies as well as to a number of psychiatric protocols. Preliminary results from stroke patients suggest that the relationships of WM structure, together with ADC and T₂, can critically improve the evaluation of cerebral ischemia progressing to infarction. An example in the evolution of stroke is shown below.

We have also used DTI to assess the anisotropy in WM of schizophrenic patients. This study showed a gray matter volume deficit but normal white matter volume in schizophrenic patients as compared to normals. Contrarily, the fractional anisotropy was shown to be lower in white matter but not in gray matter in schizophrenic patients. This suggests a compromised white matter integrity that is not discernible from structural MRI exams. The study identified a double dissociation: relative to controls, schizophrenics exhibited lower anisotropy in white matter, despite absence of a white matter volume deficit; in contrast to the white matter pattern, gray matter anisotropy did not distinguish the groups even though the schizophrenics had a significant gray matter volume deficit. The observed white matter abnormality suggests a possible compromise in the white matter integrity, which points to a potential substrate for functional disconnection or underdevelopment of the otherwise highly integrated neural networks. Thus, DTI is valuable in the evaluation of white matter health. We believe that this DTI method will prove invaluable in a wide variety of disorders that are expected to involve subtle white matter abnormalities.

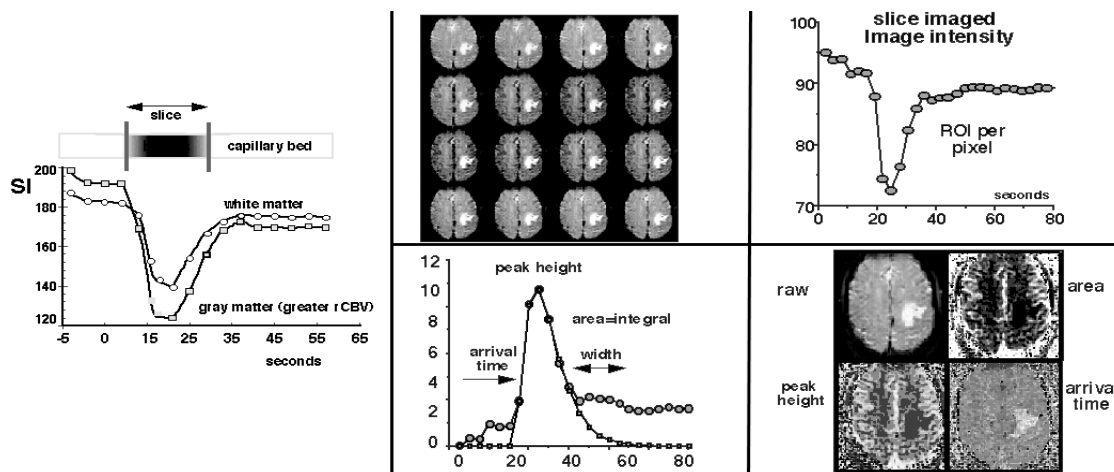
Proton Perfusion. The mechanisms of perfusion are faster than those of diffusion, by approximately two orders of magnitude. The use of MR contrast media can provide unique information in the early detection of brain perfusion changes as well as improved delineation of a perfusion-deficient or perfusion-rich region in disease states. MR contrast media, such as dysprosium chelate or iron oxide particulates, which cause regional signal losses because of magnetic susceptibility-induced T₂* shortening occurring largely in the microvasculature, have been shown to provide substantial contrast enhancement between gray and white matter as well as between ischemic and normally perfused brain. The concept of visualizing image intensity changes during the vascular transit of an injected MR contrast agent bolus requires the use of fast-scan or high-speed MR imaging. The term perfusion would in this case refer to the passage of contrast from an arterial supply to venous drainage through the cerebral microcirculation.

Bolus Tracking with T₂* Contrast Agents. The transverse relaxation time, T₂*, is used to characterize signal loss arising both from the random magnetic field fluctuations and also from coherent dephasing

associated with spatial inhomogeneity of the main magnetic field, B_0 . Since T_2^* losses result from fixed local B_0 variations, the effect can be reversed and signal restored by the use of a spin-echo instead of a gradient-echo. If high-speed or fast-scan MRI is used to obtain sequential images of the same anatomic slice, the passage of a bolus of such an agent can be tracked as a transient loss of signal intensity in the regions of arterial blood supply arising from local concentrations of the T_2^* -shortening agent. Provided that sufficient temporal resolution is achieved, the dynamics of this contrast agent transit can be used to follow the contrast transit. If the arterial blood supply is in some way compromised, a delay or reduction in the contrast-agent-induced signal loss may be observed. This provides not only a mechanism for the detection of arterial stenosis or occlusion but allows the critical assessment of delayed or collateral flow recruitment.

Since the ADC will drop when the local perfusion falls below a critical threshold, the rapid interest in mapping the correlative local tissue “perfusion” has become is certainly justified. One convenient and rapid way to do this is to inject a contrast agent with a high magnetic susceptibility such as irons or gadolinium-chelates. The presence of these agents disturb the local magnetic field, B_0 , and thus the transverse relaxation time, T_2^* , which is used to characterize signal loss arising both from the random magnetic field fluctuations and also from coherent dephasing associated with spatial inhomogeneity of the main magnetic field, B_0 (27-29). Since T_2^* losses result from fixed local B_0 variations, the effect can be reversed and signal restored by the use of a spin-echo instead of a gradient-echo. If high-speed or fast-scan MRI is used to obtain sequential images of the same anatomic slice, the passage of a bolus of such an agent can be tracked as a transient loss of signal intensity in the regions of arterial blood supply arising from local concentrations of the T_2^* -shortening agent. Provided that sufficient temporal resolution is achieved, the dynamics of this contrast agent transit can be used to follow the contrast transit. If the arterial blood supply is in some way compromised, a delay or reduction in the contrast-agent-induced signal loss may be observed. This provides not only a mechanism for the detection of arterial stenosis or occlusion but allows the critical assessment of delayed or collateral flow recruitment.

The value of bolus-tracking lies in the ability to map the underlying hemodynamics in stroke, for example, by observing the bolus transit through the microvasculature and modeling this to a gamma variate model of perfusion. From the modeling analyses, maps of the CBV and transit times can be produced (**below**).

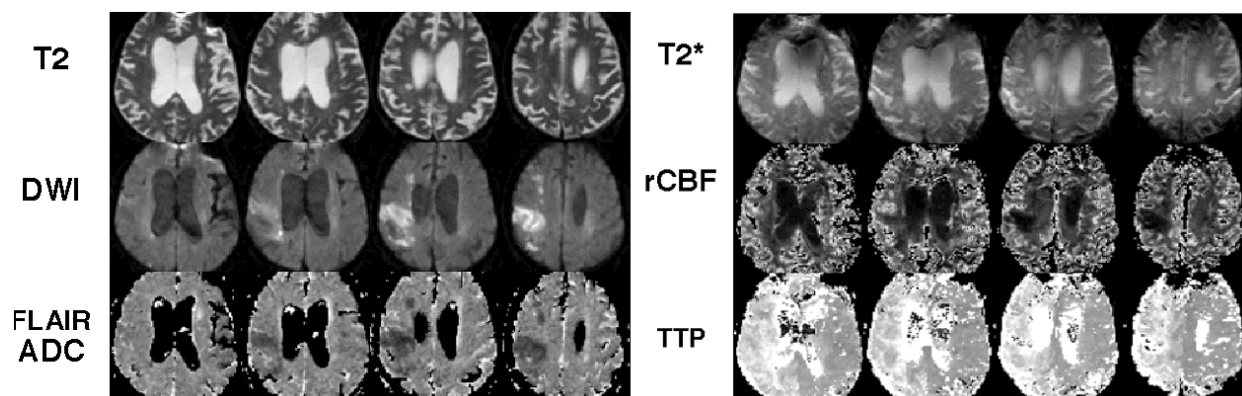


Above. Perfusion MRI using bolus tracking. As an injected bolus transits through a slice, local T_2^* decreases are observed as a transient drop in signal. This is modeled using a gamma variate analysis in which the signal measured on a pixel-by-pixel basis (upper right). This is then normalized to TE (lower left). From this, functional maps of the area under the curve (often called the rCBV), the peak effect or max, the relative transit index, and the time for bolus arrival can be mapped. These maps of hemodynamics are very useful and correlate with the DWI exams.

Perfusion imaging utilizes rapidly acquired images following a bolus injection of a contrast agent. The contrast creates a change in image intensity that can be detected as it passes through the capillary beds of the organ being imaged. Magnetic-susceptibility contrast agents such as Gadolinium-DTPA (Gd-DTPA) will assess changes in tissue perfusion by inducing a T2* shortening demonstrated as a signal loss in perfused tissue. The passage of the contrast agent can then give information on the hemodynamic status of the tissue, useful in stroke and cerebrovascular diseases. Our team of Stanford neurologists and radiologists are using these high-speed methods to better decide on the treatment of hyperacute clinical stroke. Patients are recruited within 3-6 hours of the onset of stroke, when the first effects of clinical stroke are taking place.

A combination of fast diffusion and perfusion methods creates the possibility of rapidly and repeatedly scanning patients in the MRI magnet where clinical decisions can be made directly from the images and the effects of treatment seen immediately. As these fast and efficient MR methods evolve, the idea of “from the ER to the MR” becomes a reality and will change the detection, characterization, and treatment of acute clinical stroke.

Fast MR in Stroke: Matching DWI/PWI
12 hrs, previous stroke



Above. Integrated DWI and PWI exam. At early timepoints, T2 maps do not show presence or extent of the ischemic lesions, easily seen on DWI or on ADC maps. FLAIR ADC maps are often used to suppress bright CSF from the ADC maps, which obscures the lower-than-normal lesions. Correlating with this, the PWI maps show a lower than normal rCBF (determined from the rCBV and transit maps). Note however, that the entire hemisphere shows a longer transit index, indicative of a larger perfusion or hemodynamic difficult than the focal lesion seen on DWI.

Perfusion Mapping from Spin Inversion Tagging. The observed image intensity in proton MRI depends on many parameters, such as inflow or “perfusion” of blood water protons. When blood flow to the brain delivers “fresh” blood water molecules (containing protons) into an imaged slice, this arterially-delivered water will appear very bright on an image. The greater the delivery of “perfused” water protons, the greater the intensity increase in the image. In this manner, it becomes a simple issue to actually measure the CBF from this approach, with knowledge of the blood-tissue water proton partition coefficient. Using an inflow fMRI method to detect brain response to a vascular challenge, increases in local brain function or activity will induce local increases in blood flow and thus increases in tissue image intensity.

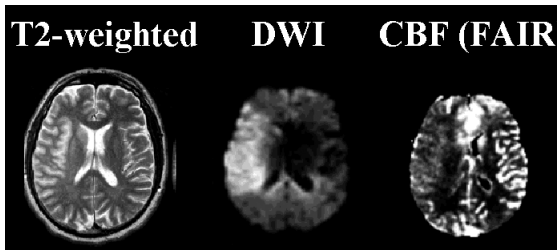


Figure. Correlation of T2-wt MRI, diffusion-weighted MRI, and an arterial inflow technique for CBF measurement (FAIR) is shown for an acute stroke case. The hyperintensity, indicative of an acute ischemic event, is seen as a perfusion deficit in the CBF map.

Diffusion Weighted Imaging (DWI) and PWI in Stroke. Existing measures of cerebral stroke severity rely primarily on neurologic exams rather than physiological imaging. It is becoming reality that diffusion-weighted imaging (DWI) coupled with perfusion-weighted imaging (PWI) will become essential to the management of stroke patients in that an integrated exam can rapidly identify the extent, location, and circulation of the relevant lesion(s) and the underlying hemodynamic behaviors responsible for the clinical symptoms. Apparent diffusion coefficient (ADC) behavior derived from DWI can uniquely monitor the clinical evolution of tissue injury from acute ischemia to chronic infarction, and provide a rapid, non-invasive means for monitoring cellular energy failure, brain edema, and cellular necrosis. The hemodynamic patterns of tissue perfusion derived from PWI can confirm existing ADC behavior, and may predict evolving ADC behavior. A 30-minute integrated protocol of existing and improved DWI, PWI, and vascular imaging MR exams can be routinely performed in the setting of acute clinical stroke.

DWI has become a useful tool for the evaluation of acute brain ischemia in that the random movements of water are rapidly diminished in regions of acute brain ischemia, which is seen as a measured decrease in the ADC mediated by water movement from the extracellular space to the intracellular space. The crucial factor responsible for the intensity changes seen on DWI is cytotoxic edema resulting from early energy depletion during acute stroke. No changes can be seen when ischemia is too limited to produce energy depletion or cytotoxic edema (6), suggesting that the ADC decreases only at CBF levels below a perfusion threshold. Because if the ADC threshold, reductions in CBF are not always matched by decreases in the ADC. The non-linearity results in the concept of the MR diffusion –to- perfusion “mismatch”.

The Perfusion-Diffusion Mismatch in Stroke: The Clinical Value of CBF. Perfusion abnormalities and measured CBF deficits are found in most ischemic stroke patients, unless reperfusion occurred prior to the PWI study (13-22). Almost all recent studies show acute perfusion abnormalities larger than the DWI lesions, leading many to believe that the “mismatch” represents viable tissue at risk, which may become recruited into the final infarct. Contrarily, if the PWI abnormality is the same size or smaller than the DWI lesion, the DWI lesion does not appear to expand significantly. With the combined use of DWI and PWI, many believe that it is possible to differentiate between patients with and without a sizable volume of potentially salvageable tissue.

The rationale for using PWI is that the perfusion thresholds for functional deficits in ischemia are slightly above that for reductions in ADC. Thus, if there is no DWI lesion, ischemia may still be the underlying cause of the patient’s symptoms, which can be revealed by PWI. In these patients (perfusion deficit, but no DWI abnormality), blood flow appears to be impaired, but not severely enough to cause energy failure in the affected region, suggesting that most or all of the affected tissue is still potentially salvageable. It is thought that restoration of blood flow which raises the CBF above the ADC threshold can reverse the DWI-observed metabolic abnormalities. In addition, in those patients with documented reperfusion via intra-arterial thrombolytic agents, a reversal of large parts of DWI lesions has been documented (18). This suggests that the ADC is reversible when CBF rises above the critical ADC threshold within a critical period of time.

The PWI-DWI “mismatch” concept has nonetheless been clinically useful. Correlations of the PWI-DWI mismatch with the clinical impression (NIHSS and ESS) find that it is the larger of the two lesion volumes that provide the better correlation with the clinical scales. The measurements of Baird, et al., (17), Tong, et al. (16), and Barber, et al. (15) demonstrated the dynamic nature of the ischemic lesion volume in stroke patients reporting that the DWI lesion volume *increased* by 200-300% when the initial PWI volume was greater than the DWI volume, but *decreased* by 40-80% when the initial PWI volume was smaller than or equivalent to the DWI volume. These three studies suggest that the initial PWI/DWI mismatches do indeed represent tissue at risk when PWI>DWI and that lesion growth represents recruitment of that tissue into the infarct.

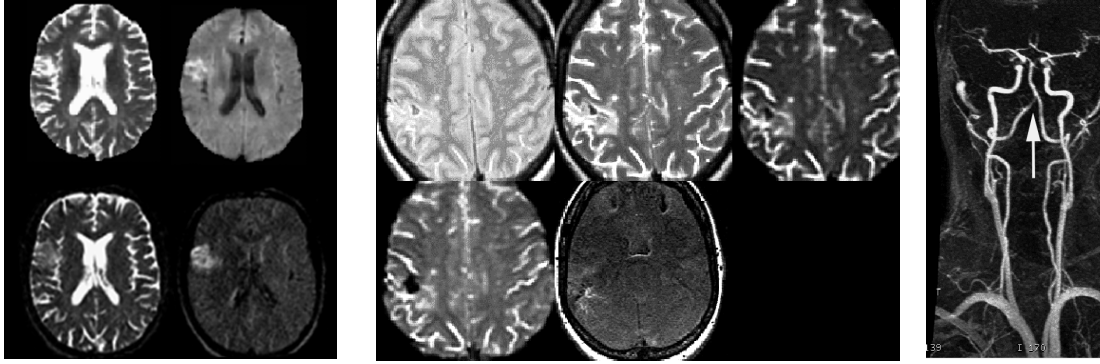
A Typical DWI PWI Stroke Protocol. In the MR exams, matching parameters are maintained wherever possible. These include FOV24 cm, TR>8000, 128x128 matrices for EPI, 1 average and slice thickness/gaps (5 mm skip 2 mm). Series of 20 slices are performed to increase coverage and reduce missed lesions in the brainstem and cord. The PWI bolus-tracking exam can acquire only a maximum of 12 slices at TR2000, however.

Table 1. Summary of DWI PWI Parameters

Sequence	Scan Tin	Role in MR Exam
GRE Sagittal Localizer	0:36	Localizer with T2* sensitivity
3D TOF Vasc SPGR MRA 60 1mm slices; 24FOV	3:34	Vascular occlusion and stenoses Oblique coverage through Circle of Willis (COW).
Fast Spin Echo (TE17/85) 256x192; 24FOV; 5/2mm	3:12	Dual Echo- low T2* sensitivity Coverage 20slices (140mm).
FSE FLAIR (2D FSE) 256x192; 24FOV; 5/2mm	2:50	Improved T2W sensitivity Coverage 20slices (140mm).
SS FSE DWI (single-shot FS) 128x128; 24FOV; 5/2mm X, Y, Z axes acquired.	1:40	DWI with SS FSE for comparison with EPI DWI Coverage 20slices (140mm). b=0 and b=500 sec/mm ² acquired.
SE EPI DWI (epi2 rev) 128x128; 24FOV; 5/2mm X, Y, Z axes acquired.	0:48	Primary EPI DWI sequence Coverage 20slices (140mm). b=0, 500, and 1000 sec/mm ² acquired.
GRE EPI (epi2 rev) 128x128, 24FOV; 5/2mm	0:06	Primary bleed screen Coverage 20slices (140mm)
Contrast-Enhanced (CE) 128x256x16; 24x48FOV;	1:20	Large FOV coronal 3DMRA bolus-tracking; 5phas seconds per phase; 0.1mmol/kg Gd
GRE EPI PWI (epi2 rev) 128x128; 24FOV; 5/2mm	1:20	Perfusion-wt bolus-tracking; 0.1mmol/kg Gd TR2000; 40phases = 80seconds.

Following a rapid GRE localizer sagittal scout series (0:36 seconds), the MRA sequence is a rapid 3D time-of-flight through the Circle of Willis (60 1mm slices from 2 slabs in 3:34 minutes). The MRA exam is used for large vessel occlusion and stenosis evaluations. The Fast Spin Echo (FSE) and FLAIR series are 256x192 resolutions with and without an initial inversion pulse (TI2200, TR10000, TE17/85, 1NEX) requiring 3:12 and 2:50 respectively.

The single-shot Fast Spin Echo (ssFSE) sequence compares favorably with the EPI DWI method in some cases (below left). The depiction of lesions in the brainstem and posterior circulation is superb at the expense of a slightly longer scan time (1.5 minutes for b=0 and b=500 sec/mm²). ADC maps are acquired from the varying b values either on-line from offline algorithms or on-line (on the scanner computer).



(Left). Comparison of single-shot EPI DWI (top) with the corresponding single-shot FSE DWI sequence (bottom) from one slice of 20 acquired. The $b=0$ and the $b=500$ sec/mm^2 images are shown. **(Middle).** MR detection of hemorrhage. Comparison of the dual-echo FSE and the T2W SE-EPI image (top row) with the corresponding GRE-EPI (TE60) and GRE (TE40) images (bottom) depict bleeds in various T2* sensitivities useful for detection as well as sizing. **(Right).** Time-resolved contrast-enhanced MRA is becoming a useful tool in depicting vascular abnormalities in stroke. Note the tightening of the basilar artery in this arterial phase angiogram.

The SE-EPI DWI sequence is a commercially available FDA-approved product. The depiction of lesions in the brainstem and posterior circulation is less accurate than the SS FSE but is much faster (0:48 seconds for the $b=0$, 500, and 1000 sec/mm^2 series, 2 averages). ADC maps are acquired as above. For both the ssFSE and the EPI DWI series, the X, Y, and Z diffusion-weighted images are averaged, effectively eliminating all observable WM anisotropy. The $b=0$, the averaged and individual diffusion-weighted images, and the averaged ADC maps are available on the scanner console screen and are filmed for reading.

The GRE EPI bleed screen exam matches the EPI DWI exam for improved hemorrhage detection. A comparison of the GRE EPI, the SE EPI, and the FSE exams (matching parameters/coverage with differing T2* sensitivities) has been found by us to be effective in detecting and characterizing the true bleed location and extent (above middle).

For vascular depiction of relative flow from the aortic arch to the Circle of Willis, we use a large FOV (24x48) coronal-plane series of rapidly-acquired 3D MR angiograms obtained over 80 seconds (5 phases) while bolus-injecting Gd-DTPA (single-dose, 0.1mmol/kg Gd). An example is shown above in (above right). This sequence is ideal for depicting carotid or basilar artery stenoses or occlusions and adds critical formation to the 3DTOF MRA and PWI exams. The flow is visualized as regional shortening of T1 and has not interfered with the first-pass T2*-shortening effect seen in the PWI series. By obtaining the contrast-enhanced MRA prior to the PWI series, both can be acquired with two separate single-dose injections.

A T2*-weighted GRE EPI pulse sequence is used for perfusion imaging with TR2000/TE60 and 12 slices, the maximum number of slices allowed by gradient duty-cycle limitations. Forty multislice image phases are obtained during bolus injection of gadolinium (single-dose, 0.1mmol/kg Gd). Bolus injections will be performed at 3ml/sec with an MR-compatible contrast power injector. The raw perfusion-weighted and calculated perfusion maps are reconstructed and displayed on the scanner console. For each slice, maps of relative blood volume (rCBV), bolus transit index (often called rMTT, as the first moment of the transit curve), and bolus arrival time (TTP in seconds) is constructed and used to look for regions of absent or markedly delayed and attenuated flow, compared to a similar region of brain in the non-ischemic hemisphere. Bolus time-to-peak (TTP) values are computed using a start time at which T2* changes are first observed in the MCA. The rMTT and the rCBF maps are further calculated from the rCBV and bolus transit index maps after measuring the arterial input behavior from either the T2*-wt EPI images. The perfusion images and maps are available for later viewing on the console.

A minimum of 20 slices is acquired for all MR exams giving coverage up to 140 mm (5mm skip 2mm slices). However, a maximum of only 12 slices can be acquired for the PWI exams yielding a coverage up to 84 mm (the twelve PWI slices are chosen to align exactly with the affected DWI EPI slices). In practice, this is sufficient, however, to cover the entire cortex where we expect observable perfusion deficits to occur. We chose the 5mm skip 2mm, 20 slices configuration to best cover the brain, allow for accurate diffusion, perfusion, and bleed comparisons.

Total exam time for the complete DWI, PWI, and bolus-tracking PWI exam is about 17 minutes. Of course, time for exam set-up, patient settling, and possible rescanning expands the MR stroke protocol to 30-45 minutes (our similar stroke protocol currently in use is presently 40 minutes only). Patient motion can affect all inter-image and intra-image studies, since series with differing b-values must be acquired for the ADC mapping. Images affected by excessive motion are presently rescanned as time allows.

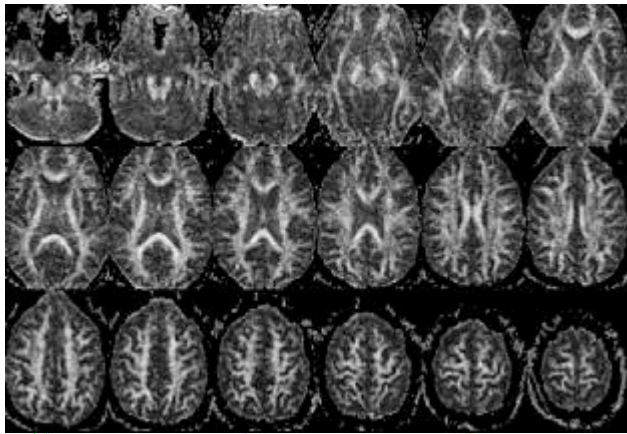
Diffusion Tensor Imaging (DTI): Mapping of the Proton Diffusion “Tensor”. In neural ordered tissue, it is thought that water diffusion is mainly influenced by the presence of myelin sheaths and intracellular structures. Perpendicular to the fiber tracts, the cholesterol-laden myelin lipid bilayers might restrict or hinder the spins from diffusing through the normally highly permeable cytomembrane. Diffusion along the fiber is more or less determined by subcellular structures, such as the endoplasmatic reticulum, mitochondria, neuro-filaments and macromolecules. In addition to that, the entire complex of axons and stabilizing tissue (i.e., glia cells, astrocytes) is also assumed to influence diffusion due to the tortuosity of proton translation, but the uniform distribution of such cells throughout the brain might render this notion less important as initially anticipated.

Diffusion “Anisotropy” Methods and Application to Neurologic Diseases. Diffusion anisotropy can be measured by determination of the so-called diffusion tensor (23-27). The tensor is essentially a map of directional vectors in 3D space, showing the preferential motion of water protons in oriented white matter. In order to acquire data for the diffusion tensor, diffusion must be measured along six or more non-collinear directions. For that purpose, a single-shot echo planar imaging (EPI) sequence was modified to allow diffusion sensitizing along any given direction. The use of fast and strong gradients (up to 30 mT/m) are needed to obtain b-values in the order of 1000 s/mm² with a diffusion time of 32ms and an effective echo time in the order of 100ms.

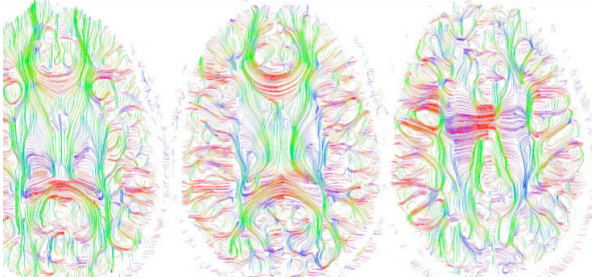
A straight-forward method of obtaining six non-collinear directions are by applying identical gradients along the following six axes combinations: $(x,y,z) = \{(1,1,0), (0,1,1), (1,0,1), (-1,1,0), (0,-1,1), (1,0,-1)\}$. This scheme has the additional advantage, that the diffusion sensitizing gradients always are applied along two axes simultaneously, thus doubling the total b-value as compared to applying gradients along one direction only. The sequence was tested for functionality (correct ADC and anisotropy values) on phantoms and volunteers. We find that using two b-values (0 and ~900) with two averages for b=0 and four averages for b=900s/mm² for a slice thickness of 5mm was appropriate to ensure an appropriate signal-to-noise ratio at 1.5Tesla.

Based on the data in the diffusion tensor, diffusion coefficients along the principal directions of the white matter fibers and eigenvectors defining the orientation of such fibers can be calculated. Software was developed for this purpose, along with software for analyzing the degree of anisotropy, given by the so-called “fractional anisotropy” (FA). The ability of DTI to discriminate between white matter (high FA, bright) and gray matter (low FA, dark) is evident. The ability of DTI to show fiber directionality and coherence is demonstrated below (right below), where lines corresponding to the principal fiber directions are shown for two enlarged regions.

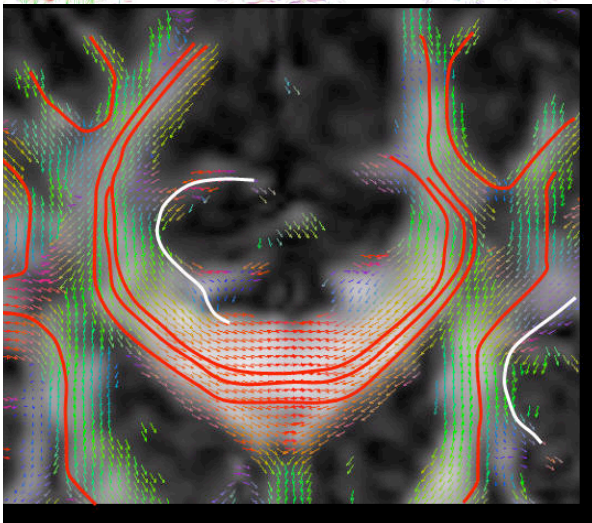
Diffusion tensor imaging can be performed on a 1.5T Signa for example (GE Signa Horizon EchoSpeed) using a spin echo EPI technique (FOV 24cm, 128x128 zero-filled to 256x256; TE/TR = 106ms/6s, 18 oblique slices, slice thickness 5mm skip 0mm). The amplitude of the diffusion-sensitizing gradients was 1.4Gauss/cm with a duration and separation of 32ms and 34ms, respectively. This resulted in a b-value of 860s/mm². Diffusion was measured along six non-collinear directions: (x,y,z) = [(1,1,0), (0,1,1), (1,0,1), (-1,1,0), (0,-1,1), (1,0,-1)]. For each gradient direction, four images were acquired and averaged. Two images with no diffusion weighting (b = 0 s/mm²) were acquired and a set of Inversion Recovery (IR) images for CSF nulling (TI ~ 2100ms) were acquired with b = 0s/mm²; these images were used to unwarp the diffusion weighted images, which resulted in a more robust unwarping than using the non-IR b=0 images. The acquired images were reconstructed prior to averaging, giving NEX = 4 for the high b-value and NEX = 2 for b = 0 s/mm². The diffusion tensor was determined for each pixel after which eigenvalues, eigenvectors and the FA was calculated.



A series of FA maps from a normal control. The fractional anisotropy yields values between 0 (perfectly isotropic diffusion) and 1 (the hypothetical case of an infinitely long and infinitely thin cylinder). In the FA map, high intensity corresponds to high anisotropy which is primarily expected in white matter, and clearly demonstrates the sensitivity of FA to white matter. The FA maps are expressed in grayscale but contain all of the directional information.

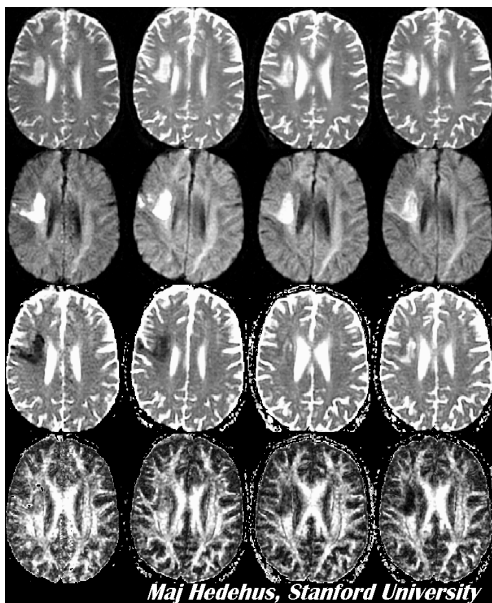


The vector information inherent in the anisotropy (such as the FA maps above) can be displayed as a color map of fiber direction and “connectivity”. In the color map, red is left-right direction, green fibers are those oriented anterior-posterior, and blue indicated fibers superior-inferior.



Once the vectors are mapped and known, one can devise novel algorithms for “tracking” the fibers from one region of the brain to another. These “fiber-tracking” tools are becoming a hot topic in brain connectivity studies using fMRI, for example. The image at left shows several red and white tracks given various “seed points”.

Diffusion Anisotropy Methods and Application to Neurologic Diseases: Diffusion Tensor Imaging (DTI) in Disease. Many groups have added DTI to a wide variety of brain MR protocols such as acute and chronic stroke, trauma, multiple sclerosis, premature babies as well as to a number of psychiatric protocols. Preliminary results from stroke patients suggest that the relationships of WM structure, together with ADC and T2, can critically improve the evaluation of cerebral ischemia progressing to infarction. An example in the evolution of stroke is shown below.



Left. Confirmed stroke imaged at 1, 2, 3 and 4 weeks post-ictum (columns 1-4). T2-weighted EPI images, diffusion weighted images and ADC maps all show the characteristic evolution of an ischemic injury to infarction: The T2-weighted hyperintensity (top row) is clearly visible at 1 week and beyond. The diffusion-weighted images (2nd row) show initial hyperintensity, corresponding to decreased diffusion that is also seen as hypointensity on the ADC maps (third row). The diffusion weighted image stays hyperintense as the T2 “shine-through” outweighs the ADC evolution from below-normal values to “pseudo-normal” and supernormal values beyond 2 weeks. The fractional anisotropy (FA, bottom row) is already decreased (0.24 ± 0.06) as compared to a corresponding region in the contralateral 0.35 ± 0.05) at one week and it continues to decrease over time (at 4 weeks: 0.08 ± 0.05 , contralateral 0.33 ± 0.07), in good correspondence with the theory of WM structural degeneration. This assessment is not apparent from either the T2 or ADC maps.

Over the past decade, diffusion weighted imaging has become an important image modality in the clinical management of stroke and for investigation of mechanisms of neuronal damage in animal models of cerebral ischemia, and the diffusion weighted images or the ADC maps are evaluated routinely. However, despite the fact that Wallerian degeneration has been shown to decrease the degree of anisotropic water motion in peripheral nerve and DTI imaging has demonstrated a decrease in anisotropy in stroke patients, tensor measures are becoming an integral part of clinical studies.

DTI has also been used to assess the anisotropy in WM of schizophrenic patients (28). This study showed a gray matter volume deficit but normal white matter volume in schizophrenic patients as compared to normals. Contrarily, the fractional anisotropy was shown to be lower in white matter but not in gray matter in schizophrenic patients. This points to a compromised white matter integrity that is not discernible from structural MRI exams. The study identified a double dissociation: relative to controls, schizophrenics exhibited lower anisotropy in white matter, despite absence of a white matter volume deficit; in contrast to the white matter pattern, gray matter anisotropy did not distinguish the groups even though the schizophrenics had a significant gray matter volume deficit. The observed white matter abnormality suggests a possible compromise in the white matter integrity, which points to a potential substrate for functional disconnection or underdevelopment of the otherwise highly integrated neural networks. Thus, DTI is valuable in the evaluation of white matter health. We believe that this DTI method will prove invaluable in a wide variety of disorders that are expected to involve subtle white matter abnormalities.

Recently, reports of water proton diffusion anisotropy abnormalities have been reported in multiple sclerosis (MS) (29-30). They concluded that DTI was able to identify MS lesions with severe tissue damage and to detect changes in the NAWM. They also indicate that DTI-derived measures are correlated with clinical disability, especially in patients with secondary progressive MS, thus suggesting a role for DTI in monitoring advanced phases of the disease. Another anticipated application of tensor mapping is in the depiction of WM changes in mild to moderate trauma (31). DTI maps the degree of directionality of water movement in white matter tracts, and is sensitive to abnormalities in the white matter integrity, composition or local ordering. Therefore, we predict that DTI can assess the degree and location of diffuse axonal injury even at the early stages in mild to moderate traumatic brain injury. Since DTI maps the composition or local ordering in white matter regions such as the corpus callosum or internal capsule, structures known to be particularly susceptible to diffuse axonal injury (DAI), we expect DTI to be sensitive to diffuse axonal injury even at early stages of axonal degradation. If so, DTI will provide a powerful tool for improved diagnosis at time of presentation and for non-invasive, longitudinal studies of diffuse axonal injury and possibly further classification of DAI with respect to anatomical location and severity. Finally, we fully anticipate that DTI will provide a much-needed look at early trauma and disease effects in the spinal cord (32-33).

Perhaps the one area where DTI is producing new results that will likely alter the field of psychiatric imaging is in the prediction of cognitive and motor performances. Klingberg, et al. (34) published an important paper in which diffusion tensor magnetic resonance imaging (MRI) was used to study the microstructural integrity of white matter in adults with poor or normal reading ability. Subjects with reading difficulty exhibited decreased diffusion anisotropy bilaterally in temporoparietal white matter. Axons in these regions were predominantly anterior-posterior in direction. No differences in T1-weighted MRI signal were found between poor readers and control subjects, demonstrating specificity of the group difference to the microstructural characteristics measured by diffusion tensor imaging (DTI). White matter diffusion anisotropy in the temporo-parietal region of the left hemisphere was significantly correlated with reading scores within the reading-impaired adults and within the control group. The anisotropy reflects microstructure of white matter tracts, which may contribute to reading ability by determining the strength of communication between cortical areas involved in visual, auditory, and language processing.

In other studies relating the DTI exam to the correlation of motor performance, the role of normal and abnormal aging have begun to explore the use of DTI. In a series of studies comparing DTI-observed changes in normal aging compared to the changes seen in suspected cases of Alzheimer's Dementia (AD), Stebbins, et al., (35-36) examined frontal-lobe FA in selected regions-of-interest (corrected for atrophic differences) in 10 younger and 10 older healthy participants. Participants were group matched for education and pre-morbid IQ. DTI was performed using a diffusion weighted single-shot spin-echo echo-planar sequence using the anatomical slice prescription from a high resolution FSE series. The DTI data were processed to provide fractional anisotropy (FA) with the group DTI data analyses performed using SPM'99. Immediately before scanning, each subject's reasoning performance was measured from a Raven's Matrices exam. The investigators found that the frontal FA was significantly reduced in older compared to younger participants ($p < .0001$). When the investigators then correlated the measured FA with cognitive skills, the reasoning performance was significantly correlated with frontal FA ($p < .0001$) while other cognitive parameters such as mental status, education and pre-morbid IQ did not significantly correlate with frontal FA. In a separate but related study (36), Urresta, et al., from the same group examined alterations in FA in Alzheimer's disease (AD). Participants consisted of 10 healthy older right-handed subjects and 10 patients with a diagnosis of probable AD. In those patients with suspected AD, the measured FA was significantly decreased ($p < 0.05$) in white matter areas corresponding bilaterally to the frontal lobes, the superior longitudinal fasciculus, and the temporal stem. Compared to the effects of normal aging on white matter integrity, these results show a further disease-induced deterioration in the microstructure of frontal and temporal lobe white matter, but not in the subcortical white matter tracts. The investigators concluded that decreases in frontal white matter microstructural integrity measured by

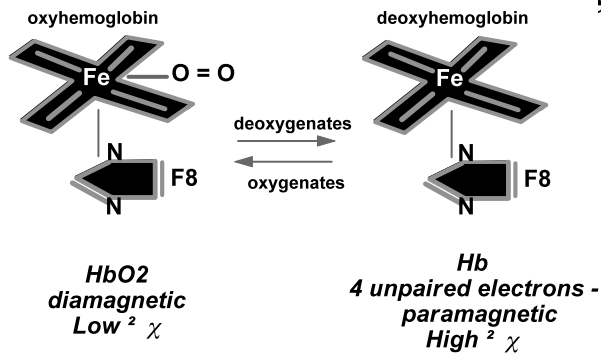
DTI FA values occur in older participants independent of atrophic changes. The correlation with reasoning performance supports a role for frontal white matter integrity in this ability.

In summary, Diffusion tensor imaging (DTI) is a promising new technique for the assessment of white matter (WM) structural integrity and connectivity. The movement of water in brain is hindered by the presence of cell membranes, myelin sheaths surrounding axons, and other structures, particularly so in white matter tracts where the apparent water diffusion is highly anisotropic, since diffusion parallel to axons and myelin bundles is considerably faster than that perpendicular to the axons. Tensors (a mathematical construct useful for describing multidimensional vector systems) are ideal for describing proton diffusion restricted by white matter tracts, by indicating the direction and the magnitude of restriction. This in turn offers an index of directional coherence of fiber tracts or integrity of cellular structure. Based on the diffusion tensor, several quantitative and absolute measures can be determined and mapped, such as the apparent diffusion coefficient (ADC), the degree of anisotropy (e.g., fractional anisotropy, FA) and measures of the correlation in orientation between a given pixel and its surrounding neighbors (e.g., the lattice anisotropy, LA). The field of DTI relating to cognitive performance, motor performance, neonatal development, demyelinating diseases, and diseases of the aging is exploding. The use of DTI will soon outstrip the use of DWI and PWI in stroke to the extent that every fMRI and MR spectroscopy will include DTI.

Functional Imaging of the Brain, fMRI. One of the most exciting recent developments in magnetic resonance imaging has been the non-invasive visualization of human brain function. Previously the exclusive domain of the technology of Positron Emission Tomography, an important subset of “functional” MRI (often denoted as *fMRI*) is now capable of mapping functional regions of the human cortex in real time during specific task activation. This is achieved using the magnetic susceptibility image contrast parameter and the fact that deoxyhemoglobin in intact erythrocytes is paramagnetic whereas oxyhemoglobin is not. Variations in regional tissue oxygenation due to changes in oxygen uptake and blood supply can then be mapped by MRI. The excitement of fMRI lies in the potential of an evolution of high-speed, non-invasive, and high-resolution exam that can track functional changes as they occur in near real-time. This capability has already become a reality for many of the newly, but rapidly-developing fMRI research centers worldwide. These centers have typically involved a number of collaborating groups from radiology, neurology, neurosurgery, psychiatry, psychology, and physics departments. Since the technique is now only about 8 years old, it is anticipated that this field will continue to quickly develop over the next decade and will involve far beyond the radiological boundaries as we know them today.

Background to fMRI. The observed image intensity in proton magnetic resonance imaging depends on many parameters, such as; proton density, T1 relaxation, T2 relaxation, blood flow, convective or diffusive processes, and spin dephasing due to tissue magnetic susceptibility variations. This last source of image contrast is of particular interest here.

It had been noted as early as 1982 that MR could non-invasively detect differences in blood oxygenation by virtue of the paramagnetic properties of deoxyhemoglobin. It was only shown recently however, that T2*-sensitive MRI could image those changes non-invasively. Today, this idea has developed into a major advance for MRI and for functional neuroimaging. In essence, MRI can detect hemodynamic responses to nearly any perturbation to the brain, such as hypoxia, hypercarbia, apnea and most importantly, task activation (30-34).



ft:

Changes in the electronic configuration of the iron in hemoglobin which occur as the molecule gives up its oxygen cause a change in the number of unpaired electron spins, and hence magnetic moment, of the iron atom.

This results in an increase in magnetic susceptibility, and decreases in T₂ and T₂* of deoxygenated blood. In brain, magnetic field gradients around the randomly oriented capillaries, due to the susceptibility difference between venous blood and tissue water, cause intravoxel spin dephasing and hence a bulk T₂* shortening in the region.

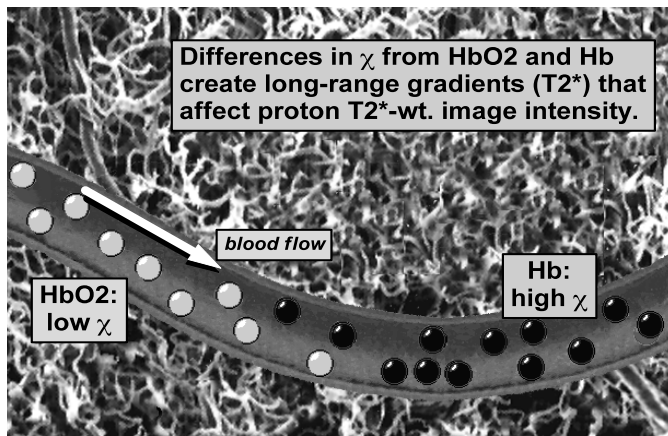


Figure. Left: Hemoglobin as an MRI contrast agent. As the oxygenation state of hemoglobin changes to deoxyhemoglobin, the iron becomes paramagnetic and thus alters the local T₂* by disturbing the local B₀. This in essence causes decreases in T₂*. As more oxygenated arterial blood is delivered to the voxel the T₂* is then increased, causing an increase in signal.

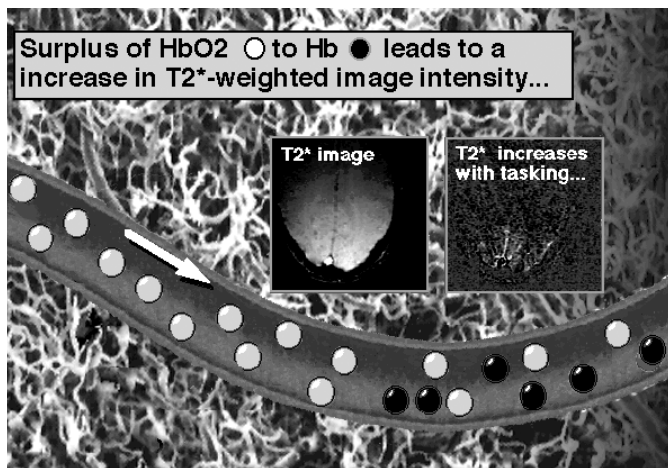


Figure. Left: As more oxygenated arterial blood is delivered to the voxel the T₂* is then increased, causing an increase in signal. Regional blood oxygenation or deoxygenation in the brain can result from changes in local or global metabolic-related oxygen uptake, and changes in blood flow. This is manifested as an increase or decrease in signal intensity in T₂* weighted images.

This effect is similar to (albeit much weaker than) the T₂* shortening effect of Gd- or Dy-chelate contrast agents and therefore leads to the idea of using deoxygenated blood as an endogenous contrast agent, sensitive to the local oxygenation state of venous blood. Regional blood oxygenation or deoxygenation in the brain can result from changes in local or global metabolic-related oxygen uptake, and changes in blood flow. This is manifested as an increase or decrease in signal intensity in T₂* weighted images.

Although these techniques do not measure tissue perfusion directly, they potentially can contribute significantly to our understanding of organ metabolism by the quantification of oxygen utilization, as well as through tissue response to various therapeutic interventions. Because more than 70% of the brain's blood lies within the capillaries and venules, the measurement of magnetic susceptibility T_2^* signal loss predominantly reflects the regional deoxygenation state of the venous system.

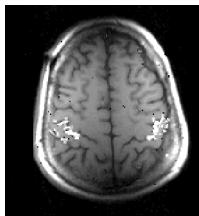


Figure. Left. fMRI BOLD map of motor cortex. As more oxygenated arterial blood is delivered to the voxel the T_2^* is then increased, causing an increase in signal. Regional blood oxygenation or deoxygenation in the brain can result from changes in local or global metabolic-related oxygen uptake, and changes in blood flow. This is manifested as an increase or decrease in signal intensity in T_2^* weighted images.

References

1. Bydder, G.M. and Young, I.R., MR imaging: clinical use of the inversion recovery sequence, *J Comput Assist Tomogr* 9: 659, 1985.
2. Noguchi K; Ogawa T; Inugami A; Toyoshima H; Sugawara S; Hatazawa J; Fujita H; Shimosegawa E; Kanno I; Okudera T. Acute subarachnoid hemorrhage: MR imaging with fluid-attenuated inversion recovery pulse sequences. *Radiology* 196(3):773-7, 1995.
3. Brant-Zawadzki MN, Atkinson D, Detrick M, Bradley WG, Scidmore G. Fluid-Attenuated Inversion Recovery (FLAIR) for Assessment of Cerebral Infarction. *Stroke* 27: 1187-1192, 1996.
4. Le Bihan, D., Breton, E., and Lallemand, D., Separation of diffusion and perfusion in intravoxel incoherent motion (IVIM) MR imaging, *Radiology* 168: 497, 1986.
5. Le Bihan, D., Breton, E., and Lallemand, D., MR imaging of intravoxel incoherent motions: application to diffusion and perfusion in neurologic disorders, *Radiology* 161: 401, 1988.
6. Le Bihan, D. and Turner, R., Diffusion and Perfusion. *Magnetic Resonance Imaging Vol. 2.*, ed. D. Stark and W. Bradley. Vol. 1, St. Louis, 1991, 56, Mosby.
7. Le Bihan, D., Douek, P., Argyropoulou, M., Turner, R., Patronas, N., and Fulham, M., Diffusion and Perfusion Magnetic Resonance Imaging of Brain Tumors, *Topics Magn Reson Imaging* 5: 25, 1993.
8. Moseley ME, Cohen Y, Mintorovitch J, Chileuitt L, Shimizu H, Kucharczyk J, Wendland MF and Weinstein PR. Early detection of regional cerebral ischemia in cats: comparison of diffusion- and T2-weighted MRI and spectroscopy. *Magnetic Resonance in Medicine* 14: 31, 1990.
9. Moseley ME, Kucharczyk J, Mintorovitch J.. Diffusion-weighted MR imaging of acute stroke: Correlation with T2-weighted and magnetic susceptibility-enhanced MR imaging in cats. *AJNR* 11: 423, 1990.
11. Mintorovitch J, Moseley ME, Chileuitt L, Shimizu H, Cohen Y, Weinstein PR. Comparison of diffusion and T2-weighted MRI for the early detection of cerebral ischemia and reperfusion in rats. *Magnetic Resonance in Medicine* 18: 39-50, 1991.
12. Minematsu K, Li L, Sotak CH, Davis MA, Fisher M. Reversible focal ischemic injury demonstrated by diffusion-weighted magnetic resonance imaging in rats. *Stroke* 23: 1304-1310, 1992.
13. Berry, I., Gigaud, M., and Manelfe, C., Experimental focal cerebral ischaemia assessed with IVIM*-MRI in the acute phase at 0.5 tesla, *Neuroradiology* 34(2): 135, 1992.
14. Knight, R., Ordidge, R., Helpen, J., and Chopp, M., Temporal Evolution of Ischemic Damage in Rat Brain by Proton Nuclear Magnetic Resonance Imaging, *Stroke* 22: 802, 1991.
15. Knight, R. Ordidge, J. Helpen, and M. Chopp, Temporal Evolution of Ischemic Damage in Rat Brain by Proton Nuclear Magnetic Resonance Imaging. *Stroke* 22: 802-804, 1991.
16. Jiang Q, Zhang ZG, Chopp M, Helpen JA, Ordidge RJ, Garcia JH, Marchese BA, Qing ZX, Knight RA: Temporal evolution and spatial distribution of the diffusion constant of water in rat brain after transient middle cerebral artery occlusion. *J Neurol Sci* 120: 123-130, 1993.

17. Knight RA, Dereski MO, Helpert JA, Ordidge RJ, Chopp M: MRI assessment of evolving focal cerebral ischemia: comparison with histopathology in rats. *Stroke* 25: 1252-1262, 1994.
18. Busza AL, Allen KL, King MD, van Bruggen N, Williams SR, and Gadian DG. Diffusion-weighted imaging studies of cerebral ischemia in gerbils. Potential relevance to energy failure. *Stroke* 23 (11): 1602-12, 1992.
19. Chien, D., Buxton, R.B., Kwong, K.K., Brady, T.J., and Rosen, B.R., MR diffusion imaging of the human brain, *J Comput Assist Tomogr* 14(4), 514, 1990. See also: Chien D, Kwong KK, Gress DR, Buonanno FS, Buxton RB, Rosen BR. MR diffusion imaging of cerebral infarction in humans. *AJNR* 13: 1097-1102 (1992).
20. Warach, S., Chien, D., Li, W., Ronthal, M., and Edelman, R.R., Fast magnetic resonance diffusion-weighted imaging of acute human stroke, *Neurology* 42(9): 1717, 1992.
21. Warach, S., J. Gaa, B. Siewert, P. Wielopolski, and R. Edelman, Acute Human Stroke Studied by Whole Brain Echo Planar Diffusion-weighted Magnetic Resonance Imaging. *Annals of Neurology* 37(2): 231-238, 1994.
22. Warach S, Dashe JF, Edelman RR. Clinical outcome in ischemic stroke predicted by early diffusion-weighted and perfusion magnetic resonance imaging: a preliminary analysis. *Journal of Cerebral Blood Flow and Metabolism* 16(1): 53-9, 1996.
23. de Crespigny A, Yenari M, Enzmann D, Marks M, Moseley M. Navigated spin-echo diffusion imaging of human stroke. *Magnetic Resonance in Medicine* 33: 720-728, 1995.
24. Marks M, de Crespigny, A, Lentz D, Enzmann, D, Albers, G, Moseley, M. Navigated Spin-echo Diffusion Imaging of Acute and Chronic Stroke. *Radiology* In press, 1996.
25. Moseley ME, Butts K, Yenari M, Marks M, de Crespigny A. Clinical Aspects of DWI. *NMR in Biomedicine* 8: 387-396, 1996.
26. D. Spielman, K. Butts, A. de Crespigny, M. Moseley, Diffusion-Weighted Imaging of Clinical Stroke, *International Journal of NeuroRadiology* In Press, 1996.
27. Villringer A, Rosen BR, Belliveau, J W, Ackerman JL, Lauffer RB, Buxton RB, Chao YS, Wedeen V, and Brady TJ. Dynamic imaging with lanthanide chelates in normal brain: contrast due to magnetic susceptibility effects, *Magnetic Resonance in Medicine* 6: 164, 1988.
28. Rosen BR, Belliveau JW, Buchbinder BR, McKinstry RC, Porkka LM, Kennedy DN, Neuder MS, Fisel CR, Aronen HJ, Kwong KK. Contrast agents and cerebral hemodynamics, *Magnetic Resonance in Medicine* 19(2): 285, 1991.
29. Rosen BR, Belliveau JW, and Chien D. Perfusion imaging by nuclear magnetic resonance, *Magn Reson Quarterly* 5(4): 263, 1989.
30. Thulborn, K., Waterton, J., Matthews, P., and Radda, G., Oxygenation dependence of the transverse relaxation time of water protons in whole blood at high field., *Biochem Biophys Acta*, 714, 265, 1982.
31. Turner, R., LeBihan, D., Moonen, C., Despres, D., and Frank, J., Echo Planar Time Course MRI of Cat Brain Oxygenation Changes, *Magn Reson Med*, 22, 159, 1991.
32. Ogawa, S., Lee, T., Nayak, A., and Glynn, P., Oxygenation sensitive contrast in MRI in rodent brain at high #2. magnetic fields., *Magn Reson Med*, 14, 68, 1990.
33. Kwong, K., Belliveau, J., Chesler, D., and Goldberg, I., Dynamic Magnetic Resonance Imaging of Human Brain Activity During Primary Sensory Stimulation., *Proceed Nat Acad Sciences*, 89, 5675-5679, 1992.
34. Bandettini, P., Wong, E., Hinks, R., Tikofsky, R., and Hyde, J., Time course EPI of human brain function during task activation., *Magn Reson Med*, 25, 390, 1992.